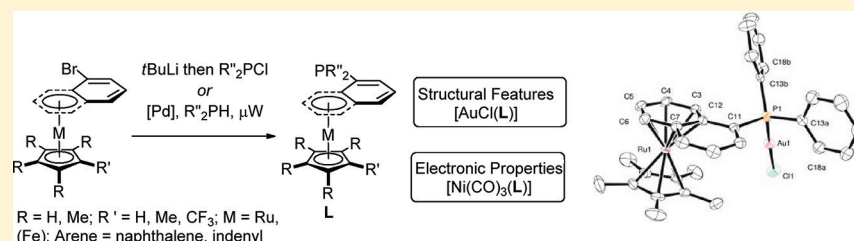


Functionalization of Planar Chiral Fused Arene Ruthenium Complexes: Synthesis, X-ray Structures, and Spectroscopic Characterization of Monodentate Triarylphosphines

Philipp Buchgraber, Audrey Mercier, Wee Chuan Yeo, Céline Besnard, and E. Peter Kündig*

Department of Organic Chemistry, University of Geneva, Quai Ernest Ansermet 30, 1211 Geneva 4, Switzerland

S Supporting Information



ABSTRACT: The efficient functionalization of planar chiral ruthenium naphthalene—and ruthenium indenyl—scaffolds is reported. Mild reaction conditions employing microwave heating have been developed for the derivatization of sensitive cationic naphthalene ruthenium complexes. In particular, a series of novel planar chiral monodentate phosphines and their gold(I) complexes have been synthesized and fully characterized by NMR spectroscopy and X-ray crystallography. Furthermore, the electronic properties of these phosphines (L) have been evaluated via the infrared CO stretching frequencies of the corresponding Ni(CO)₃(L) complexes, providing valuable insight for the design and application of these chiral ligands in asymmetric catalysis.

INTRODUCTION

Tertiary phosphines are arguably the most important ancillary ligands in transition-metal chemistry and catalysis. A variety of derivatives have been designed and fine-tuned in terms of steric and electronic properties to realize highly active and selective catalytic reactions. While phosphines featuring elements of central or axial chirality are among the most widely employed chiral ligands,¹ the inherent planar chirality of unsymmetrically substituted metal arene complexes or metallocenes constitutes another prominent motif for chiral phosphines. In particular, ligands based on a chiral ferrocenyl core have found widespread applications in asymmetric catalysis.² A synergistic combination of two elements of chirality (central and planar chiralities) usually accounts for their notable success in promoting high asymmetric induction.³ However, ferrocene ligands exhibiting only planar chirality could also provide excellent enantioselectivities in various transformations, demonstrating the prominent role of this stereogenic element.^{2h,4} In addition to the ubiquitous ferrocenyl chiral ligands, (arene)-tricarbonylchromium complexes have also been explored, albeit to a lesser extent, and proved to induce effective chiral environments.⁵ In sharp contrast, the homologous ruthenium sandwich scaffold has received scarce attention.⁶

We have recently succeeded in accessing planar chiral fused arene chromium, ruthenium, and iron complexes in moderate to high enantioselectivities through two complementary Pd-catalyzed asymmetric transformations (Scheme 1).^{7,8} These desymmetrization processes paved the way for the development

of valuable classes of compounds. Indeed, the resulting planar chiral backbones are well suited for further derivatizations, owing to the presence of a remaining bromide atom. Herein, we present our synthetic efforts to functionalize the scaffolds obtained after the hydrogenolysis reaction (Scheme 2). A special emphasis is placed on the development of a new subset of chiral phosphines, as well as on the evaluation of their structural and electronic properties in view of further applications in asymmetric catalysis.

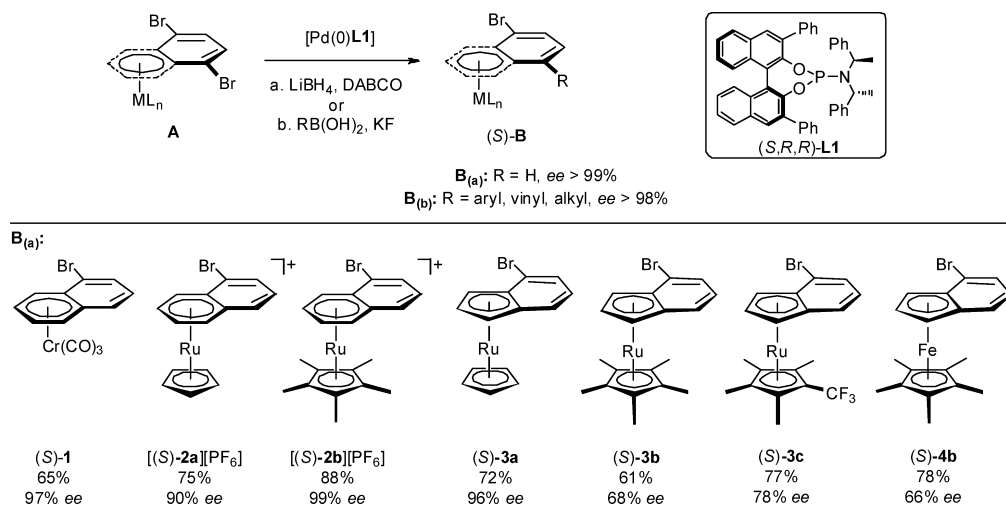
RESULTS AND DISCUSSION

Synthesis. In analogy with chromium complex **1**,⁹ cyclopentadienyl(indenyl)ruthenium and iron complexes **3a–c** and **4b** are compatible with bromine/lithium exchange conditions. As such, functionalization with various chlorodiphosphine derivatives as electrophiles allowed for an expedient access to neutral planar chiral phosphines **5–8** (Scheme 3).¹⁰ Importantly, the use of *n*BuLi in diethyl ether was not appropriate¹¹ and clean reactions were only obtained after treatment with 2 equiv of *t*BuLi at low temperature. The sequential trapping of the resulting organolithium species with different R₂P-Cl derivatives provided phosphines with diverse electronic and steric properties in moderate to good yields. Products **5–8** proved stable in their solid state but slowly oxidized in solution.

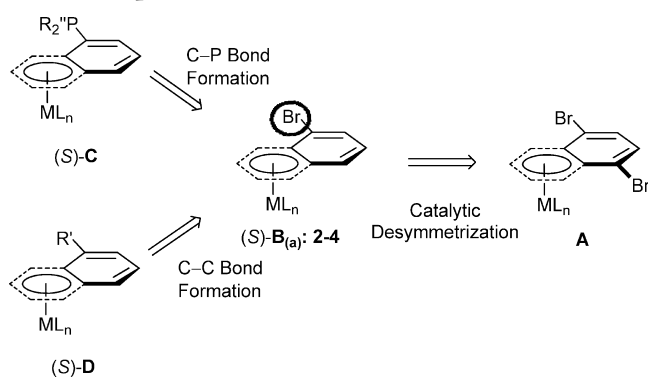
Received: September 27, 2011

Published: November 1, 2011

Scheme 1. Access to Planar Chiral Complexes via Pd-Catalyzed Desymmetrization Processes



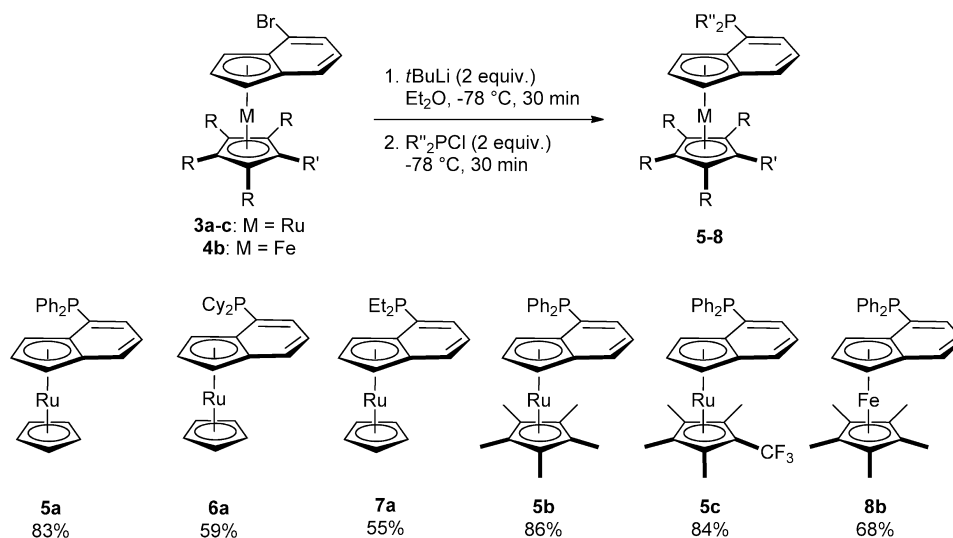
Scheme 2. Synthetic Approach to Functionalized Planar Chiral Complexes



In stark contrast, the high electrophilicity of the $[\text{RuCp}]^+$ unit in complexes **2** precluded the use of strongly basic and nucleophilic reagents such as *t*BuLi. Indeed, nucleophilic attack onto the coordinated arene or reduction to $[\text{Ru}(\text{I})]$ via single-electron transfer could occur under such conditions.^{12,13} On

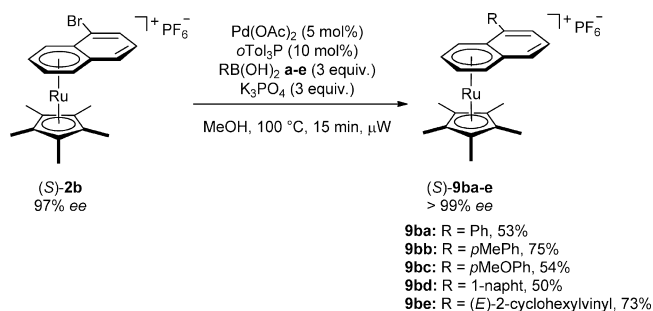
the other hand, the great activating effect of the metal fragment was ideally suited for the development of transition-metal-catalyzed cross-coupling reactions. As demonstrated for the hydrogenolysis reaction, the oxidative addition of the Pd(0) species into the $\text{C}_{\text{Ar}}\text{-Br}$ bond was significantly accelerated, owing to the decrease of π -electron density. Therefore, transition-metal-catalyzed C–P bond-forming reactions were envisaged to realize the challenging sought-after transformation under mild conditions.¹⁴ Palladium,¹⁵ nickel,¹⁶ and copper-catalyzed¹⁷ C–P cross-coupling reactions are emerging in importance for the preparation of phosphine ligands. However, these transformations are significantly more challenging than related carbon–heteroatom (C–O, C–N) cross-coupling reactions. Aryl iodides as coupling partners, high temperatures (100–110 °C), and long reaction times (several hours or days) are generally required. In contrast to such harsh conditions, the use of secondary phosphine–boranes allowed for the development of ambient processes.^{15e,f} However, the use of acetonitrile as solvent and amine bases prevented their application to ruthenium(II) arene complexes. To the best of our knowledge, only two protocols (enabling an asymmetric C–P bond

Scheme 3. Neutral Indenylphosphines Prepared via Bromine/Lithium Exchange



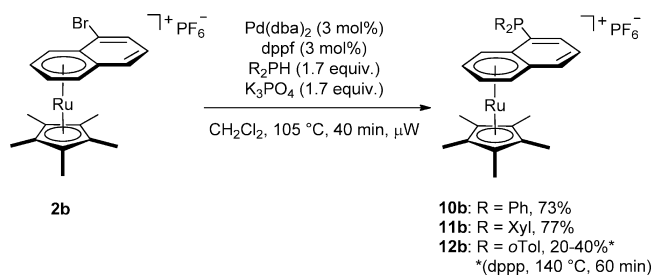
forming reaction) describe the use of unprotected secondary phosphines at room temperature.^{15c,d} Moreover, the use of microwave heating has recently been introduced to circumvent the long reaction times associated with this type of coupling.¹⁸ The latter precedents¹⁸ combined with the results obtained in the microwave-promoted Suzuki–Miyaura cross-coupling of complex **2b**^{7b} prompted us to implement a similar strategy for the targeted C–P bond construction. Indeed, the use of microwave heating appeared as an essential tool to streamline the coupling of **2b** with various boronic acids. The reaction performed best in methanol using Pd(OAc)₂/oTol₃P as catalyst and K₃PO₄ as base at 100 °C.¹⁹ Reaction times were dramatically shortened, thereby reducing side reactions and allowing for the isolation of the coupled products in moderate to good yields (Scheme 4).

Scheme 4. Suzuki–Miyaura Cross-Coupling of 2b with Representative Boronic Acids



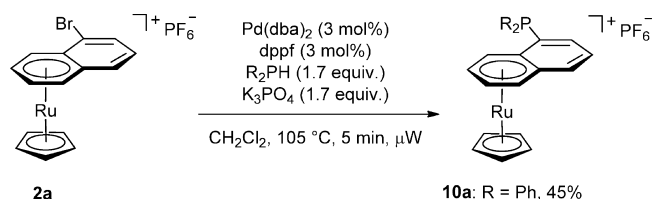
Not unexpectedly, after reaction of **2b** with Ph₂PH in the presence of Pd(dba)₂/*t*Bu₃P and DABCO in DME at room temperature for 4 h, only trace amounts of the desired product could be identified by ³¹P NMR analysis of the crude mixture (δ_{P} −13.3 ppm, CDCl₃), along with many other signals. Microwave irradiation (100 °C, 10 min) of a mixture containing the air-stable borane adduct Ph₂PH·(BH₃), **2b**, Pd(OAc)₂/*t*Bu₃P, and K₂CO₃ in DME gave significantly more conversion into the corresponding phosphine. Interestingly, the cross-coupled product was mainly deprotected under these conditions. Other diphenylphosphine coupling partners, such as Ph₂PSiMe₃, Ph₂PK, and Ph₂P(O)H, resulted in failure. Pleasingly, the best set of conditions appeared with the use of unprotected diphenylphosphine in conjunction with Pd(dba)₂ and dppf as catalyst precursors and K₃PO₄ as base in CH₂Cl₂. Optimal conditions were refined upon scale up (0.5 mmol), leading to complete conversion of the starting material within 40 min of microwave heating at 105 °C and reducing side product formation to a minimum (Scheme 5).²⁰ After

Scheme 5. Pd-Catalyzed C–P Cross-Coupling of Complex 2b



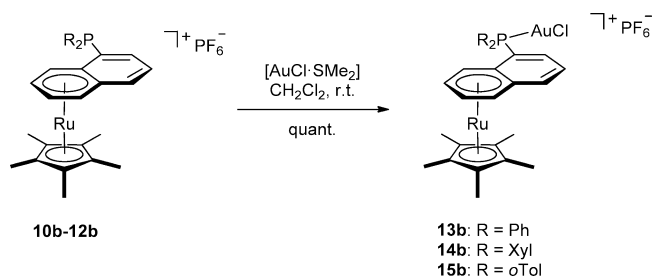
purification by flash chromatography to remove a small unidentified impurity (δ_{P} +35 ppm, CD₂Cl₂), phosphine **10b** (R = Ph) could be isolated in 73% yield. Reaction in the presence of bis(3,5-dimethylphenyl)phosphine²¹ as coupling partner proceeded equally well and afforded phosphine **11b** (R = Xyl) in 77% yield. In sharp contrast, the use of the sterically more demanding di-*o*-tolylphosphine²² resulted in partial conversion under such conditions. Increasing both catalyst loading (10 mol %) and reaction time (80 min) resulted only in decomposition. With NiCl₂(dppp) as catalyst, the starting material remained unchanged. In contrast, when Pd(dba)₂ was used in combination with dppp as ligand at 140 °C, complete consumption of the substrate could be achieved after 1 h, albeit with substantial decomposition. As such, pure phosphine **12b** was isolated in variable yields (20–40%). Moreover, the C–P cross-coupling of the less robust [Ru($\eta^5\text{-Cp}$)($\eta^6\text{-5-bromonaphthalene}$)](PF₆)[−] (**2a**) under standard conditions resulted in a messy mixture of products. Control experiments disclosed that complex **2a** was unstable in the presence of diphenylphosphine (3% of decomplexation after 1 h at room temperature). Therefore, reduction of the microwave irradiation time to 5 min limited the decomposition process and allowed for the isolation of phosphine **10a** (R = Ph) in a satisfactory yield of 45% (Scheme 6).

Scheme 6. Pd-Catalyzed C–P Cross-Coupling of Complex 2a



Gold Complexes. With the purpose of evaluating the performance of the synthesized phosphines as chiral ligands in asymmetric catalysis, their coordination chemistry was first explored. Reaction of phosphines **10b–12b** with [AuCl·SMe₂] in CH₂Cl₂ gave the corresponding gold(I) complexes **13b–15b** in quantitative yields as yellow solids after precipitation in pentane (Scheme 7).

Scheme 7. Synthesis of Gold(I) Complexes



Structural Analysis. Suitable crystals for X-ray diffraction studies were obtained by slow diffusion of diethyl ether into dichloromethane solutions at 4 °C. Crystallographic data for [Ru($\eta^5\text{-Cp}^*$)($\eta^6\text{-5,8-dibromonaphthalene}$)](PF₆)[−] (**16b**) and phosphines (\pm)-**11b** and (\pm)-**12b**, as well as for gold complexes (*S*)-**13b** and (\pm)-**14b** are summarized in Table 1. Selected bond distances, bond angles, and torsion angles are collected in Table 2. The ORTEP views of the complexes are

Table 1. Crystallographic Data for Complexes 11b, 12b, (S)-13b, 14b, and 16b

	11b	12b	(S)-13b	14b	16b
chem formula	C ₃₆ H ₄₀ PRu·PF ₆ ·CH ₂ Cl ₂	C ₃₄ H ₃₆ PRu·PF ₆ ·0.5CH ₂ Cl ₂	C ₃₂ H ₃₂ PRuAuCl·PF ₆	C ₃₆ H ₄₀ PRuAuCl·PF ₆	C ₂₀ H ₂₁ Br ₂ Ru·PF ₆
mol wt	834.65	764.13	926.03	982.11	667.3
cryst syst	monoclinic	monoclinic	orthorhombic	triclinic	orthorhombic
space group	<i>P</i> 2 ₁ / <i>c</i>	<i>P</i> 2 ₁ / <i>c</i>	<i>P</i> 2 ₁ 2 ₁ 2 ₁	<i>P</i> $\bar{1}$	<i>Pca</i> 2 ₁
<i>a</i> (Å)	12.430(2)	12.063(4)	8.8175(3)	9.7785(5)	16.9376(9)
<i>b</i> (Å)	13.083(3)	29.793(9)	16.5684(9)	14.0984(7)	8.3480(4)
<i>c</i> (Å)	24.751(5)	11.307(6)	21.9915(9)	14.8098(7)	15.1736(11)
α (deg)	90	90	90	67.035(4)	90
β (deg)	90.99(3)	112.60(2)	90	78.308(4)	90
γ (deg)	90	90	90	74.928(4)	90
<i>V</i> (Å ³)	4024.4(14)	3752(3)	3212.8(2)	1803.41(17)	2145.5(2)
<i>Z</i>	4	4	4	2	4
<i>d</i> (g/cm ⁻³)	1.378	1.352	1.914	1.809	2.066
<i>T</i> (K)	200	293	200	200	150
radiation type			Mo <i>K</i> α		
μ (mm ⁻¹)	0.65	0.63	5.271	4.701	4.587
<i>T</i> _{min} , <i>T</i> _{max}	0.860, 0.900	0.71, 1.00	0.18, 0.45	0.45, 0.83	0.396, 0.496
no. of rflns measd	34 662	49 948	22 487	36 082	25 524
no. of indep rflns	10 221	7316	7409	12 344	4626
no. of rflns obsd (<i>I</i> / σ > 2)	6559	4770	6076	6746	3734
<i>R</i> _{int}	0.033	0.052	0.038	0.058	0.036
no. of params	550	534	389	424	271
no. of restraints	216	270	0	0	0
refinement			full matrix on <i>F</i> ²		
<i>R</i> [<i>F</i> ² > 2 σ (<i>F</i> ²)]	0.038	0.045	0.020	0.0354	0.018
<i>R</i> _w (<i>F</i> ²)	0.060	0.110	0.034	0.0822	0.018
<i>S</i>	1.03	1.04	1.07	1.13	1.25
$\Delta\rho_{\text{min}}$, $\Delta\rho_{\text{max}}$ (e Å ⁻³)	-0.40, 0.50	-0.56, 0.56	-2.26, 2.15	-2.54, 1.00	-0.52, 0.54
Flack param			-0.015(3)		-0.005(6)

Table 2. Selected Distances (Å) and Angles (deg)

entry		11b	12b	13b	14b
Bond Lengths					
1	Ru1–C3	2.218(3)	2.219(4)	2.230(4)	2.215(6)
2	Ru1–C4	2.222(3)	2.218(4)	2.217(4)	2.202(6)
3	Ru1–C5	2.221(3)	2.229(5)	2.226(4)	2.228(6)
4	Ru1–C6	2.189(3)	2.222(5)	2.201(4)	2.182(6)
5	Ru1–C7	2.257(3)	2.273(4)	2.250(4)	2.254(6)
6	Ru1–C12	2.274(3)	2.304(4)	2.295(4)	2.295(5)
7	P1–C11	1.832(4)	1.839(4)	1.828(4)	1.811(6)
8	P1–C13a	1.830(3)	1.848(5)	1.814(4)	1.812(6)
9	P1–C13b	1.833(3)	1.838(5)	1.805(4)	1.808(5)
10	Au1–P1			2.2341(10)	2.2308(14)
Bond Angles					
11	C13b–P1–C13a	101.85(13)	103.6(2)	108.18(18)	105.2(3)
12	C13b–P1–C11	102.67(14)	101.8(2)	104.91(18)	105.0(2)
13	C13a–P1–C11	101.07(13)	102.3(2)	104.49(18)	106.6(3)
14	Au1–P1–C11			113.58(13)	113.12(18)
15	Au1–P1–C13a			111.04(14)	111.94(19)
16	Au1–P1–C13b			113.99(14)	114.27(19)
Dihedral Angles					
17	C18a–C13a–P1–C11	108.41(3)	89.49(4)	96.14(3)	94.95(5)
18	C18b–C13b–P1–C11	-166.42(2)	-167.16(4)	-135.66(3)	-150.94(5)
19	C12–C11–P1–C13a	174.27(2)	177.13(4)	164.96(3)	162.08(4)
20	C12–C11–P1–C13b	69.32(2)	70.18(4)	51.25(3)	50.75(5)
21	C3–C12–C11–P1	-2.90(3)	-1.34(7)	9.64(5)	7.56(8)
22	Au1–P1–C11–C12			-73.90(3)	-74.46(5)

depicted in Figures 1–3. For clarity, the same enantiomer is shown in Figures 2 and 3.

The crystal structure of [Ru(η^5 -Cp*)(η^6 -5,8-dibromonaphthalene)][PF₆] (**16b**) is a good starting point

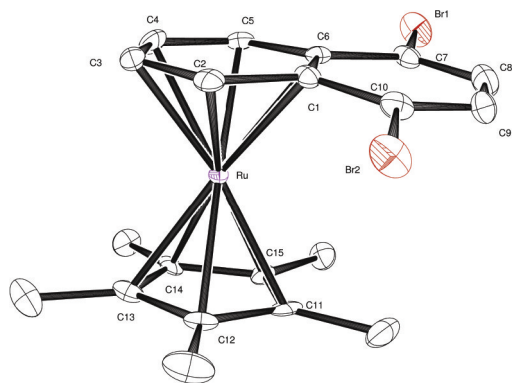


Figure 1. ORTEP drawing of the molecular structure of $[\text{Ru}(\eta^5\text{-Cp}^*)(\eta^6\text{-5,8-dibromonaphthalene})][\text{PF}_6]$ (**16b**). Thermal ellipsoids are set to 50% probability. Hydrogen atoms and PF_6 anion are omitted for clarity. Selected bond distances (Å) and dihedral angles (deg): Ru–C1 = 2.255(5), Ru–C2 = 2.215(5), Ru–C3 = 2.226(5), Ru–C4 = 2.213(5), Ru–C5 = 2.225(5), Ru–C6 = 2.274(5), Ru–C11 = 2.189(5), Ru–C12 = 2.192(5), Ru–C13 = 2.177(5), Ru–C14 = 2.178(5), Ru–C15 = 2.175(4); C2–C1–C10–Br2 = $-1.1(7)$, C5–C6–C7–Br1 = $+6.1(7)$.

for comparison (Figure 1). Ruthenium is bound in an η^6 fashion to the less substituted ring with slightly elongated Ru–C1 and Ru–C6 distances (2.255(5) and 2.274(5) Å, respectively) compared to the Ru–C2 to Ru–C5 bonds (2.215(5), 2.226(5), 2.213(5), 2.225(5) Å), which are all routine for ruthenium(II) arene complexes.²³ Such slippage toward the less substituted side of the η^6 -arene complex is well-known in the literature.²⁴ Similarly, the Cp^* is bound in an η^5 fashion with relatively average Ru–C distances (2.175(4)–2.192(5) Å).^{23a} The two planes of the sandwich are almost parallel (1.4°). The two arene rings of the naphthalene are twisted, as indicated by the dihedral angles C2–C1–C10–Br2 ($-1.1(7)^\circ$) and C5–C6–C7–Br1 ($+6.1(7)^\circ$).

The structures of **11b** and **12b** are of low quality, due to a strong disorder observed for the counterion, the Cp^* ring, and the solvent molecules (Figure 2). For both compounds, the Cp^* and the PF_6 anion were modeled using two molecules.

Distances and angles were restrained to ideal values. Restraints were also applied to anisotropic displacement parameters. Although this disorder affects the R values, the bonding situation within the relevant cationic part of the complex is unambiguous. The aryl substituents on phosphines **11b** and **12b** showed elongated anisotropic parameters, which are compatible with a pendulum movement with center C13 and axis C13–C16.²⁵

Despite highly disordered Cp^* rings, all Ru– C_{Cp^*} (ranging from 2.127(8) to 2.210(6) Å for **11b** and 2.097(17) to 2.166(13) Å for **12b**) and Ru– C_{naphth} distances (Table 2, entries 1–6) are routine and similar to those of the parent $[(\eta^5\text{-Cp}^*)(\eta^6\text{-5,8-dibromonaphthalene})]$ (**16b**). The two structures are essentially superimposable and differ only in the twist of the aryl rings (Table 2, entries 17 and 18). The torsion angles between the naphthalene ring system and the aryl rings are $174.27(2)$ and $69.32(2)^\circ$ for **11b** and $177.13(4)$ and $70.18(4)^\circ$ for **12b** (Table 2, entries 19 and 20). The phosphorus atom is slightly bent down toward the $[\text{RuCp}^*]^+$ moiety (**11b**, $-2.90(3)^\circ$; **12b**, $-1.34(7)^\circ$; Table 2, entry 21). The bond lengths and angles around the phosphorus atom are routine for an sp^3 -hybridized trivalent phosphorus (Table 2, entries 7–9 and 11–13) and compare well with those of the parent 1-naphthyldiphenylphosphine (PPh_2Np , not shown), devoid of the $[\text{RuCp}^*]^+$ moiety (1.8284(17)–1.8387(17) Å, $101.85(7)$ – $104.12(7)^\circ$).^{17c} Interestingly, the latter displayed a similar arrangement of the aryl rings (torsion angles C12–C11–P1–C13a/b = $178.5/75.8^\circ$), demonstrating the small influence of the η^6 coordination of the $[\text{RuCp}^*]^+$ moiety on the solid-state structure.

The two gold(I) complexes **13b** and **14b** are almost superimposable (Figure 3). The Ru– C_{Cp^*} (ranging from 2.167(4) to 2.193(4) Å for **13b** and 2.165(6) to 2.186(6) Å for **14b**) and Ru– C_{naphth} distances (Table 2, entries 1–6) are in the usual range observed for related complexes. The overall orientation of the phosphorus atom is close to that of phosphines **11b** and **12b**, as indicated by the similar dihedral angles C12–C11–P1–C13a/b ($164.96(3)/51.25(3)^\circ$ for **13b**; $162.08(4)/50.75(5)^\circ$ for **14b**; Table 2, entries 19 and 20). Such

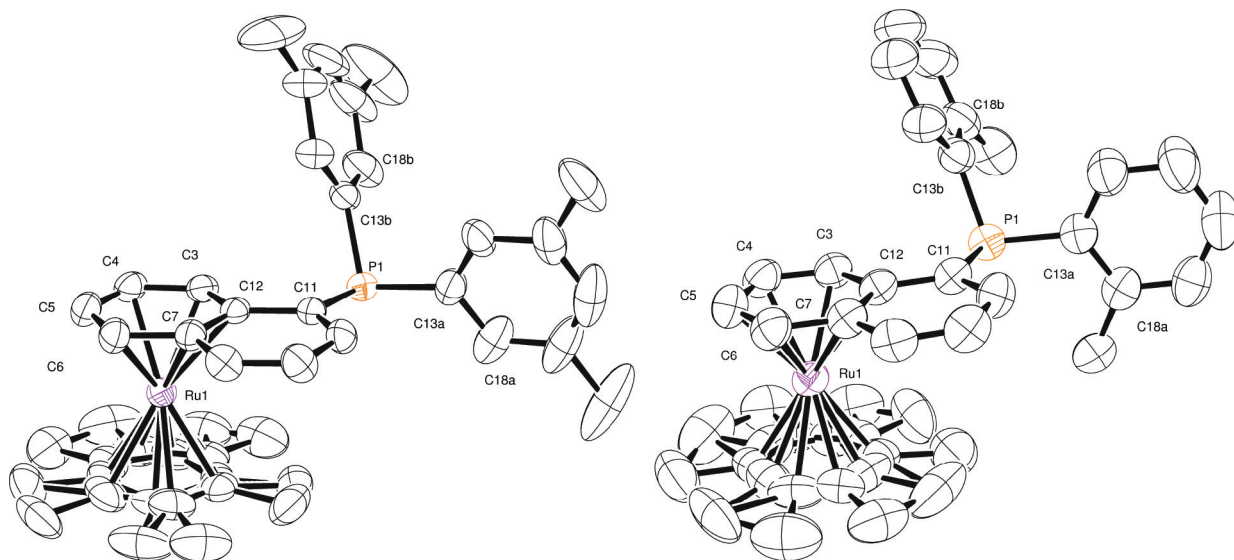


Figure 2. ORTEP drawings of the molecular structures of **11b** (left) and **12b** (right). Thermal ellipsoids are set to 60% probability. Hydrogen atoms and PF_6 anion are omitted for clarity.

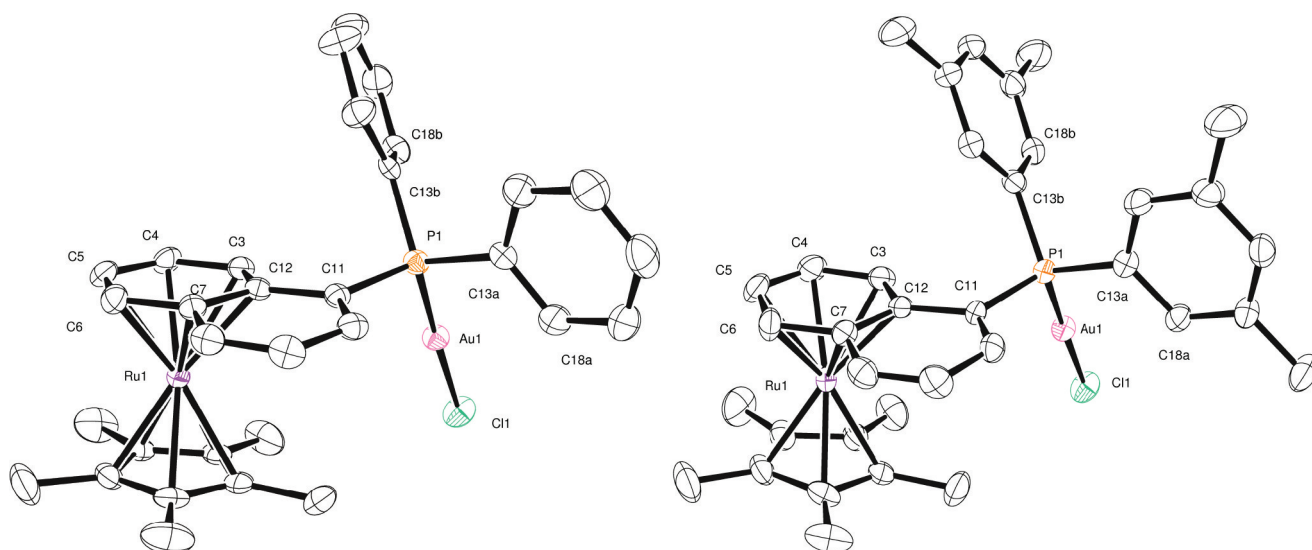


Figure 3. ORTEP drawings of the molecular structures of (*S*)-**13b** (left) and **14b** (right). Thermal ellipsoids are set to 60% probability. Hydrogen atoms and PF₆[−] anion are omitted for clarity.

arrangement implies that the coordinated [AuCl] moiety points toward the [RuCp*]⁺ unit (Table 2, entry 22). However, distortion of the tetrahedral coordination sphere of the phosphorus is observed, as characterized by the bond angles around the phosphorus varying from 104.49(18)° to 113.99(13)° for **13b** and from 105.0(2)° to 114.27(19)° for **14b** (Table 2, entries 11–16). Furthermore, the [RuCp*]⁺ moiety is bent away from the P1–Au1–Cl1 axis, which results in dihedral angles C3–C12–C11–P1 of +9.64(5)° for **13b** and +7.56(8)° for **14b** (Table 2, entry 21) and an increased angle between the η⁶-arene and η⁵-Cp* planes (**13b**: 3.3°; **14b**: 4.3°).

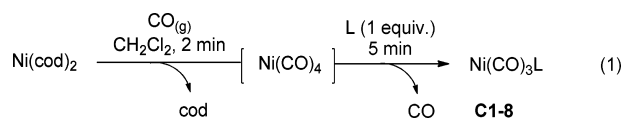
NMR Spectroscopic Studies. The NMR spectra of **10b**–**15b** deserve some comments. As already shown for the parent [Ru(η⁵-Cp*)(η⁶-5,8-dibromonaphthalene)][PF₆]⁺ (**16b**), selective coordination of the [RuCp*]⁺ fragment onto the less substituted ring causes a high-field shift of the four-proton spin system of ca. 2 ppm, whereas the singlet corresponding to the two protons of the uncoordinated ring is only shifted by 0.3 ppm as compared to that of the free 1,4-dibromonaphthalene.²⁶ Similarly, the ¹³C NMR chemical shifts (δ_C) of the π-coordinated carbons are in the range 85.4–97.4 ppm, whereas δ_C shifts for the free ligand are in the range 124.8–134.9 ppm.²⁶ Such coordination chemical shifts (Δδ) to higher field are typical for π complexes of Ru(II).²⁷ Similar observations apply to [Ru(η⁵-Cp*)(η⁶-5-bromonaphthalene)][PF₆]⁺ (**2b**). However, the situation becomes more complex for the phosphine complexes **10b**–**12b**. High-resolution²⁸ HSQC and HMBC experiments in combination with classical 1D and 2D NMR experiments were essential to unambiguously attribute all ¹³C signals (Table S1, Supporting Information). Analogously, δ_C for the π-coordinated carbons are in the range 83.5–100.0 ppm, whereas the uncoordinated carbons have typical aromatic carbon shifts (128.3–144.3 ppm). The aryl rings on the phosphines are diastereotopic, and the symmetrically substituted **10b** (Ar = Ph) and **11b** (Ar = Xyl) show local C₂ symmetry, indicating a free rotation along the P–C axis. The J_{C,P} coupling constant pattern of the diastereotopic aryl rings in **10b** and **11b** correlates well with the data reported for Ph₃P.²⁹ J_{C,P} coupling in the naphthyl part is somewhat disturbed by the π-coordinated [RuCp*]⁺ moiety. Interestingly, the methyl

groups of the Cp* unit feature a J_{C,P} coupling of ca. 3 Hz. This long-range J_{C,P} coupling through a metal center has not been reported and is not observed in the corresponding gold complexes **13b** and **14b**. Coordination of gold(I) chloride affects in particular the ¹³C chemical shifts and J_{C,P} coupling constants in the vicinity, whereas the π-coordinated carbons remain unchanged. In contrast to the free phosphines **10b** and **11b**, which have well-correlated ¹³C NMR spectra, δ_C and J_{C,P} in the corresponding gold complexes **13b** and **14b** are random (Table S2). Similar observations were made for [AuCl-(PPh₂Np)].³⁰ ¹H and ³¹P NMR signals of gold complex **15b**, bearing the sterically more demanding *o*-tolyl substituents, are broad, precluding a full assignment. As for the neutral indenylphosphines, a similar analysis can be made (Table S3).³¹

Tolman Electronic Parameter (TEP). Evaluation of the electronic properties of this series of novel phosphines appeared essential for the design and application of these motifs as chiral ligands in asymmetric catalysis. The importance of quantifying steric and electronic effects of ligands has been recognized in pioneering studies by Tolman on tertiary phosphines³² and has had a crucial impact on homogeneous catalysis. In particular, Tolman's lasting achievement consists of the introduction of the electronic parameter ν, known as the Tolman electronic parameter (TEP). This tool has been used to quantify the electron-donor ability of a wide range of phosphorus ligands and, more recently, of NHCs.³³ The TEP corresponds to the frequency of the A₁ carbonyl mode of a Ni(CO)₃L complex and represents a direct probe to gauge the electronic characteristics of ligand L. Indeed, replacement of one CO in the Ni(CO)₄ complex by a tertiary phosphine increases the electron density at the metal center, which compensates by more π back-bonding into CO π* orbitals. This synergistic phenomenon further strengthens the remaining Ni–CO bonds and weakens the C–O bond, implying a decrease of the CO stretching frequency by an amount depending on the net donating ability of the phosphorus ligand.³⁴ However, the high toxicity of Ni(CO)₄ fostered the search for alternative methods.³⁵ As such, a plethora of analogous transition-metal carbonyl complexes were investigated (e.g. Rh, Cr, Mo, W, Ir),³⁶ and considerable efforts were invested to assess the donor properties by means of

computational methods.³⁷ In addition to CO stretching frequencies, ¹³C NMR chemical shifts of these metal carbonyl complexes, as well as C–P and M–P coupling constants, were notably studied for the same purpose. Despite the inconvenience of handling Ni(CO)₄, the simplicity and reliability of the experimental measurement coupled with the large number of reference values available prompted us to choose Tolman's original system for our study.

Ni(CO)₃L complexes were prepared according to the procedure of Tolman,³⁸ except that Ni(CO)₄ was conveniently generated in situ by ligand exchange from Ni(cod)₂ with CO(g) in CH₂Cl₂. Upon disappearance of the slight yellow color of Ni(cod)₂, ensuring complete formation of Ni(CO)₄, a solution containing phosphine L was added and immediate evolution of CO was observed (eq 1, Scheme 8). The



complexes were not isolated but directly analyzed by means of FT-IR spectroscopy. The recorded carbonyl stretching frequencies of complexes C1–C8 were referenced to the Tolman scale using Ni(CO)₃(Ph₃P) as reference ($\nu_{\text{CO}}(\text{A}_1)$ 2068.9 cm⁻¹).³² The corrected values are presented in Table 3 together with those of representative Ni(CO)₃(R₃P) complexes to allow for a direct comparison. Figure 4 provides a clear overview of the electron richness of the new planar chiral phosphines. All these characteristic stretching frequencies in hand allowed for a comparative study of the electronic properties of the eight selected phosphines. In particular, we were intrigued by the impact of the coordinated transition-metal fragment on the electron-donating ability of the complexes, since no data relative to this effect have been reported yet.

From Table 3 and Figure 4, it appears that the phosphine family covers a wide range of electronic properties, the carbonyl stretches falling between 2060.3 and 2074.6 cm⁻¹. The neutral cyclopentadienyl(indenyl)ruthenium complexes **5a–c** and iron complex **8b** are very similar in basicity and compare well with triarylphosphines such as *o*Tol₃P (Table 3, compare entries 1–4 and 11). The coordination of a neutral [RuCp] fragment results in slightly more electron-donating ligands than the parent PPh₃ (Table 3, compare entries 1–4 and 9). Electronic communication from the cyclopentadienyl ring to the phosphorus atom is reflected by the distinct TEP values within complexes **5a–c** (Table 3, entries 1–3). Incorporation of cyclohexyl substituents on the phosphorus generates the most basic phosphine of the series (**6a**, Table 3, entry 5).

Table 3. $\nu_{\text{CO}}(\text{A}_1)$ Values for [Ni(CO)₃L] Complexes Measured in CH₂Cl₂

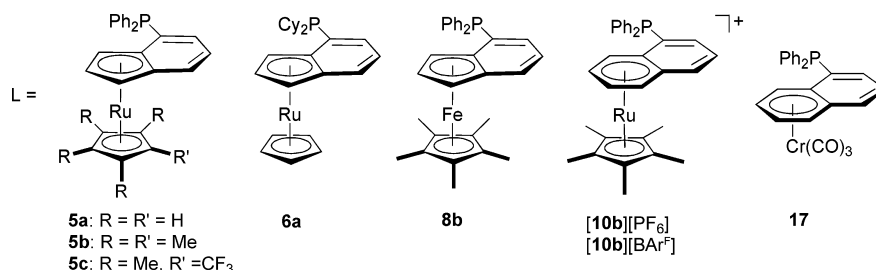
entry	ligand	complex	$\nu_{\text{CO}}(\text{A}_1)^a$ (cm ⁻¹)
1	5a	C1	2066.7
2	5b	C2	2066.1
3	5c	C3	2067.3
4	8b	C4	2066.5
5	6a	C5	2060.3
6	17	C6	2071.1
7	[10b][PF ₆]	C7	2073.3
8	[10b][BAR ^F]	C8	2074.6
9 ^b	Ph ₃ P	Ni(CO) ₃ (Ph ₃ P)	2068.9
10 ^b	<i>t</i> Bu ₃ P	Ni(CO) ₃ (<i>t</i> Bu ₃ P)	2056.1
11 ^b	<i>o</i> Tol ₃ P	Ni(CO) ₃ (<i>o</i> Tol ₃ P)	2066.6
12 ^b	Ph ₂ (EtO)P	Ni(CO) ₃ (Ph ₂ (EtO)P)	2071.2
13 ^b	(EtO) ₃ P	Ni(CO) ₃ ((EtO) ₃ P)	2076.3

^aCorrected experimental values using [Ni(CO)₃(Ph₃P)] as reference (lit., $\nu_{\text{CO}}(\text{A}_1)$ 2068.9 cm⁻¹; exptl, $\nu_{\text{CO}}(\text{A}_1)$ 2069.5 cm⁻¹). ^bFrom ref 32.

On the other hand, the strongly electron-withdrawing effect of the [Cr(CO)₃] entity significantly depletes electron density from the phosphorus center (Table 3, entry 6). As such, complex **17** and phosphinite Ph₂(EtO)P are electronically comparable (Table 3, compare entries 6 and 12). Of particular interest is the effect of the [RuCp*]⁺ fragment in phosphine **10b**⁺. The positive charge overrides completely the strong electron-donating character of the [RuCp*] moiety, resulting in the least electron-rich phosphine of the family (Table 3, entry 7). Furthermore, a strong counterion effect is observed for **10b**⁺. Replacing the PF₆ anion by the more lipophilic BAR^F considerably decreases the electron density of the system ($\Delta(\text{TEP}) = 1 \text{ cm}^{-1}$; Table 3, compare entries 7 and 8).

The TEPs of the neutral indenyl complexes **5a–c** and **8b** deserve some further comment. During the desymmetrization studies of [Ru(η^5 -Cp*)(η^5 -4,7-dibromoindene)],^{7b,c} the otherwise efficient catalyst system afforded the hydrogenolysis product in a moderate 68% ee. At first, it was surmised that this effect might be of electronic origin caused by the increased electron donation of the [RuCp*] fragment. To support this hypothesis, the complex featuring an η^5 -C₅Me₄CF₃ ligand was evaluated. The latter possesses similar electronic properties of Cp and the steric bulk of Cp*.³⁹ An intermediate enantiomeric excess of 78% was obtained, indicating that both electronic and steric factors are operative. A similar conclusion could be drawn from the TEP analysis of the corresponding diphenylphosphine complexes **5a–c**. On the basis of Tolman's reasoning that only inductive effects are responsible for the electronic properties, TEP values for **5a,c** should be identical. However, a $\Delta(\text{TEP})$ value of 0.6 cm⁻¹ was found experimentally. This indicates that

Scheme 8. Set of Phosphines Considered in the Study



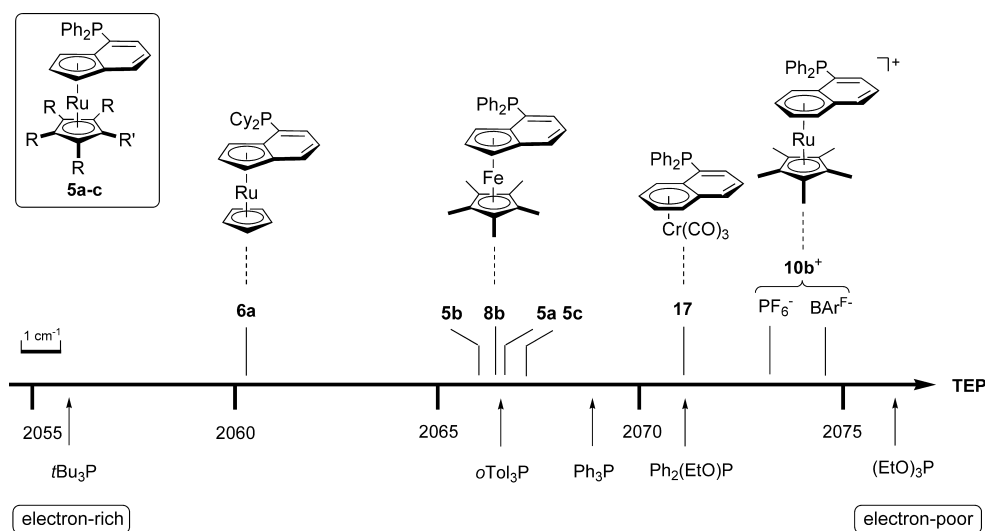


Figure 4. Comparison of Tolman electronic parameters.

Tolman's simple assumption of purely additive inductive effects on the net donor ability is not valid in such a sterically demanding environment.⁴⁰

CONCLUSION

In conclusion, we have reported efficient and useful transformations of sensitive ruthenium complexes. The planar chiral building blocks were transformed into valuable derivatives either by metalation/electrophilic quenching sequences or by Pd-catalyzed cross-coupling reactions. The latter took advantage of the strong activation of the system toward oxidative addition. Particularly, we developed mild reaction conditions that exploit the benefits of microwave heating to address the challenging functionalization of cationic ruthenium complexes. Of particular importance was the development and characterization of new planar chiral monodentate phosphines. Evaluation of their structural features by X-ray crystallography and their electronic properties through TEP values provided valuable insight for further applications in asymmetric catalysis, which will be the subject of further studies.

EXPERIMENTAL SECTION

General Remarks. All reactions and manipulations were carried out under an inert atmosphere of nitrogen using an inert gas/vacuum double-manifold line and standard Schlenk techniques unless otherwise stated. Solvents were dried by passing through activated Al₂O₃ using a Solvtek purification system or by following standard procedures.⁴¹ When required, the solvents were degassed by three successive freeze–thaw–pump cycles. Commercially available chemicals were purchased from Fluka, Aldrich, Pressure Chemicals, and Acros and used as received unless otherwise stated. The following metal complexes and reagents were synthesized according to literature procedures: (*S*)-**1–4**,^{7c} [Ru(η^5 -Cp*)(η^6 -5,8-dibromonaphthalene)]-[PF₆]⁻ (**16b**),^{7c} [Cr(CO)₃(η^6 -5-diphenylphosphinonaphthalene)] (**17**),⁹ Pd(dba)₂,⁴² AuCl·SMe₂,⁴³ bis(3,5-dimethylphenyl)phosphine, and di-*o*-tolylphosphine.⁴⁴

Flash column chromatography was performed using silica gel 60 (32–63 mesh, Brunschwig) or neutral alumina (50–200 μ m, Acros). Analytical thin-layer chromatography (TLC) was performed on precoated aluminum plates (silica gel 60 F₂₅₄, Merck; aluminum oxide, POLYGRAM ALOX N/UV₂₅₄). Microwave reactions were performed in a Biotage Initiator SW apparatus. ¹H, ¹³C, ³¹P, and ¹⁹F NMR spectra were recorded on 500, 400, and 300 MHz Bruker Avance spectrometers in the solvent indicated. ¹H and ¹³C NMR

chemical shifts (δ) are quoted in ppm relative to SiMe₄ (residual CHCl₃, δ _H 7.26 ppm; CDCl₃, δ _C 77.05 ppm; residual CHDCl₂, δ _H 5.32 ppm; CD₂Cl₂, δ _C 53.9 ppm; residual C₆H₅D₅, δ _H 7.15 ppm; C₆D₆, δ _C 128.0 ppm). ³¹P NMR chemical shifts are referenced to H₃PO₄ as external standard. ¹⁹F NMR chemical shifts are referenced to CFCl₃ as external standard. Coupling constants *J* are quoted in Hz. Infrared spectra were recorded on a Perkin–Elmer 1650 FT-IR spectrometer using a diamond ATR Golden Gate sampling. Electron impact (EI) HRMS mass spectra were obtained using a Finnigan MAT 95 instrument operating at 70 eV. Electrospray ionization (ESI) HRMS analyses were measured on a VG Analytical 7070E instrument. Optical rotations were measured at 20 °C on a Perkin–Elmer 241 polarimeter using a quartz cell (*l* = 10 cm) with a Na high-pressure lamp (λ 589 nm). Melting points were measured in open capillary tubes on a Büchi 540 apparatus and are uncorrected. Elemental analyses were carried out by H. Eder and K. L. Buchwalder from the University of Geneva. X-ray structure determinations were performed using a STOE IPDS 2 image-plate diffractometer with graphite-monochromated Mo *K* α radiation (λ 0.710 69 Å). Specimens of suitable size and quality were selected and mounted onto a nylon loop. The structures were solved either by direct methods using sir 92⁴⁵ (for **13b** and **14b**) and sir 97⁴⁶ (for **16b**) or by the charge-flipping method using superflip⁴⁷ (for **11b** and **12b**); all the structures could be solved by either method. Subsequent refinement on *F*² was realized using the CRYSTALS software package⁴⁸ (for **11b–14b**) or with XTAL⁴⁹ (for **16b**). Details about the refinement can be found in Table 1 as well as in the Supporting Information.

General Procedure for the Metalation/Electrophilic Trapping Sequence. The monohalide complex was dissolved in diethyl ether, and the resulting solution was cooled to –78 °C. *t*BuLi (2 equiv) was added dropwise. After the mixture was stirred for 30 min at this temperature, R₂PCL (2 equiv) was added. The resulting mixture was stirred for 30 min and passed through a short pad of silica gel under N₂ (pentane/CH₂Cl₂ 9/1). The crude product was purified by column chromatography on silica gel. The enantiomeric purity of the phosphine was determined by HPLC on chiral stationary phase.

[Ru(η^5 -Cp)(η^5 -4-(diphenylphosphino)indene)] (**5a**). Prepared according to the general procedure from [Ru(η^5 -Cp)(η^5 -4-bromoindene)] (**3a**, 96% ee (*S*), 412 mg, 1.14 mmol), *t*BuLi (2.26 M, 1.01 mL, 2.28 mmol), and Ph₂PCL (423 μ L, 2.28 mmol) in diethyl ether (11 mL). A yellow solid was obtained after purification by flash chromatography (pentane, then pentane/CH₂Cl₂ 9/1) (440 mg, 83% yield, 96% ee (*S*)). *R*_f = 0.6 (pentane/CH₂Cl₂ 9:1). Mp: 68–70 °C. [α]_D = +849° (*c* = 0.33, CHCl₃). ¹H NMR (500 MHz, CD₂Cl₂): δ 7.46–7.32 (m, 11H), 6.72 (dd, *J* = 8.5, 6.7 Hz, 1H), 6.53 (t, *J* = 6.5 Hz, 1H), 5.24–5.20 (m, 2H), 4.57 (t, *J* = 2.4 Hz, 1H), 4.11 (s, 5H). ¹³C NMR (125 MHz, CD₂Cl₂): δ 137.2 (d, *J* = 10.7 Hz), 136.5 (d, *J* = 10.6

Hz), 135.6 (d, $J = 13.8$ Hz), 134.7 (d, $J = 20.5$ Hz), 134.1 (d, $J = 19.7$ Hz), 129.4, 129.0, 128.9 (d, $J = 3.9$ Hz), 128.8 (d, $J = 6.9$ Hz), 128.7 (d, $J = 7.3$ Hz), 128.4, 122.6 (d, $J = 2.7$ Hz), 95.5 (d, $J = 26.0$ Hz), 91.9 (d, $J = 5.6$ Hz), 73.2, 70.5, 66.3 (d, $J = 11.5$ Hz), 66.0 (d, $J = 1.6$ Hz). ^{31}P NMR (162 MHz, CD_2Cl_2): $\delta -13.1$. IR: 3053, 2962, 2921, 2851, 1738, 1584, 1474, 1432, 1331, 1300, 1260, 1178, 1100, 1026, 995, 855, 808, 773, 764, 741, 724, 692 cm^{-1} . HRMS (ESI) for $\text{C}_{26}\text{H}_{22}\text{PRu} [\text{M} + \text{H}]^+$: calcd 467.0497, found 467.0468. Anal. Calcd for $\text{C}_{26}\text{H}_{21}\text{PRu}$ (465.49): C, 67.09; H, 4.55. Found: C, 65.84; H, 4.52.

[Ru($\eta^5\text{-Cp}^*$)($\eta^5\text{-4-(diphenylphosphino)indene}$)] (5b). Prepared according to the general procedure from $[\text{Ru}(\eta^5\text{-Cp}^*)(\eta^5\text{-4-bromindene})]$ (**3b**, 67% ee (*R*), 368 mg, 0.85 mmol), *t*BuLi (2.4 M, 724 μL , 1.70 mmol), and Ph_2PCL (315 μL , 1.70 mmol) in diethyl ether (15 mL for solubility reasons). A yellow solid was obtained after purification by flash chromatography (pentane, then pentane/ CH_2Cl_2 9/1) (391 mg, 86% yield, 67% ee (*R*)). $R_f = 0.3$ (pentane/ CH_2Cl_2 9:1). Mp: 126–128 °C. $[\alpha]_D = -791^\circ$ ($c = 0.50$, CHCl_3). ^1H NMR (500 MHz, CD_2Cl_2): δ 7.43–7.25 (m, 10H), 7.12 (dt, $J = 8.6$, 0.8 Hz, 1H), 6.71 (ddd, $J = 8.6$, 6.6, 0.9 Hz, 1H), 6.28 (ddd, $J = 6.5$, 5.6, 0.8 Hz, 1H), 4.75 (td, $J = 2.9$, 1.0 Hz, 1H), 4.72–4.70 (m, 1H), 4.36 (t, $J = 2.5$ Hz, 1H), 1.70 (s, 15H). ^{13}C NMR (125 MHz, CD_2Cl_2): δ 137.4 (d, $J = 11.3$ Hz), 136.8 (d, $J = 11.8$ Hz), 135.1 (d, $J = 20.1$ Hz), 134.5 (d, $J = 12.7$ Hz), 134.5 (d, $J = 20.2$ Hz), 129.2 (d, $J = 18.1$ Hz), 128.9 (d, $J = 7.2$ Hz), 126.5, 125.8, 120.8 (d, $J = 0.9$ Hz), 94.5 (d, $J = 24.6$ Hz), 91.8 (d, $J = 6.1$ Hz), 83.1, 77.3, 68.9 (d, $J = 11.0$ Hz), 68.7 (d, $J = 2.1$ Hz), 11.1 (d, $J = 1.6$ Hz). ^{31}P NMR (162 MHz, CD_2Cl_2): $\delta -13.4$. IR: 3053, 2966, 2903, 1739, 1587, 1475, 1434, 1378, 1329, 1299, 1091, 1069, 1033, 1024, 814, 805, 765, 744, 721, 604 cm^{-1} . HRMS (ESI) for $\text{C}_{31}\text{H}_{32}\text{PRu} [\text{M} + \text{H}]^+$: calcd 537.1281, found 537.1279. Anal. Calcd for $\text{C}_{31}\text{H}_{31}\text{PRu}$ (535.62): C, 69.51; H, 5.83. Found: C, 69.44; H, 6.07.

[Ru($\eta^5\text{-Cp}^*$)($\eta^5\text{-4-(diphenylphosphino)indene}$)] (5c). Prepared according to the general procedure from $[\text{Ru}(\eta^5\text{-Cp}^*)(\eta^5\text{-4-bromindene})]$ ((\pm) -**3c**, 46.7 mg, 0.96 mmol), *t*BuLi (2.28 M, 90 μL , 0.21 mmol), and Ph_2PCL (26 μL , 0.15 mmol) in diethyl ether (2 mL). A yellow solid was obtained after purification by flash chromatography (pentane, then pentane/ CH_2Cl_2 5/1) (49 mg, 84% yield). Mp: 105–106 °C. ^1H NMR (500 MHz, CD_2Cl_2): δ 7.41–7.27 (m, 10H), 7.15 (dt, $J = 8.5$, <1 Hz, 1H), 6.77 (ddd, $J = 8.7$, 6.6, 0.8 Hz, 1H), 6.35 (ddd, $J = 6.1$, 5.4, 0.8 Hz, 1H), 5.01 (td, $J = 2.7$, 0.9 Hz, 1H), 4.88–4.86 (m, 1H), 4.53 (t, $J = 2.5$ Hz, 1H), 1.94 (q, $^5J_{\text{HF}} = 0.9$ Hz, 3H), 1.68 (s, 3H), 1.65 (q, $^5J_{\text{HF}} = 1.3$ Hz, 3H), 1.56 (s, 3H). ^{13}C NMR (125 MHz, CD_2Cl_2): δ 136.9 (d, $J = 11.0$ Hz), 136.2 (d, $J = 11.7$ Hz), 134.9 (d, $J = 20.2$ Hz), 134.8 (d, $J = 14.0$ Hz), 134.5 (d, $J = 20.3$ Hz), 129.4, 129.2, 128.9 (d, $J = 7.3$ Hz), 128.9 (d, $J = 7.3$ Hz), 128.6 (q, $J = 27.0$ Hz), 127.1, 126.2, 122.2, 95.6 (d, $J = 24.3$ Hz), 92.8 (d, $J = 6.0$ Hz), 86.0, 85.7, 82.1 (q, $^3J_{\text{CF}} = 1.4$ Hz), 81.8 (q, $^3J_{\text{CF}} = 1.4$ Hz), 77.7, 76.2 (q, $^2J_{\text{CF}} = 35.8$ Hz), 69.8 (d, $J = 11.0$ Hz), 69.2 (d, $J = 1.9$ Hz), 11.7 (pent, $J_{\text{CF}} \approx J_{\text{CF}} \approx 2$ Hz), 10.5 (q, $^4J_{\text{CF}} = 1.8$ Hz), 10.4 (d, $J = 2.7$ Hz), 9.7 (d, $J = 3$ Hz). ^{31}P NMR (202 MHz, CD_2Cl_2): $\delta -13.3$. ^{19}F NMR (470 MHz, CD_2Cl_2): $\delta -53.2$. IR: 2962, 2908, 2872, 1454, 1424, 1380, 1334, 1261, 1241, 1189, 1098, 1035, 1015, 743, 728, 693 cm^{-1} . HRMS (ESI) for $\text{C}_{31}\text{H}_{29}\text{F}_3\text{PRu} [\text{M} + \text{H}]^+$: calcd 591.0996, found 591.1038.

[Ru($\eta^5\text{-Cp}$)($\eta^5\text{-4-(dicyclohexylphosphino)indene}$)] (6a). Prepared according to the general procedure from $[\text{Ru}(\eta^5\text{-Cp})(\eta^5\text{-4-bromindene})]$ (**3a**, 96% ee (*S*), 54 mg, 0.15 mmol), *t*BuLi (1.89 M, 152 μL , 0.30 mmol), and $\text{C}_6\text{H}_5\text{PCL}$ (66 μL , 0.30 mmol) in diethyl ether (1.5 mL). A yellow solid was obtained after purification by flash chromatography (pentane, then pentane/ CH_2Cl_2 1/1) (42 mg, 59% yield, 96% ee (*S*)). Mp: 79–81 °C. $[\alpha]_D = +872^\circ$ ($c = 0.2$, CHCl_3). ^1H NMR (400 MHz, CDCl_3): δ 7.39 (d, $J = 8.4$ Hz, 1H), 6.92 (t, $J = 6.0$ Hz, 1H), 6.79 (dd, $J = 8.4$, 6.0 Hz, 1H), 5.48 (t, $J = 2.4$ Hz, 1H), 5.24 (t, $J = 2.4$ Hz, 1H), 4.64 (t, $J = 2.4$ Hz, 1H), 4.23 (s, 5H), 1.02–1.92 (m, 20H). ^{13}C NMR (100 MHz, CDCl_3): δ 132.5 (d, $J = 1.6$ Hz), 127.9, 127.7, 122.1, 98.3 (d, $J = 26.4$ Hz), 91.9 (d, $J = 5.9$ Hz), 72.9, 70.1, 68.9 (d, $J = 14.0$ Hz), 65.8 (d, $J = 1.4$ Hz), 33.7 (d, $J = 12.8$ Hz), 31.7 (d, $J = 10.1$ Hz), 31.1 (d, $J = 14.7$ Hz), 30.1 (d, $J = 13.8$ Hz), 29.7 (d, $J = 15.6$ Hz), 28.6 (d, $J = 3.7$ Hz), 27.8 (d, $J = 12.9$ Hz), 27.4 (d, $J = 6.4$ Hz), 27.3 (d, $J = 3.7$ Hz), 27.2 (d, $J = 3.7$ Hz), 26.7, 26.5. ^{31}P

NMR (162 MHz, CDCl_3): $\delta -10.1$. HRMS (ESI) for $\text{C}_{26}\text{H}_{34}\text{PRu} [\text{M} + \text{H}]^+$: calcd 479.1436, found 479.1430.

[Ru($\eta^5\text{-Cp}$)($\eta^5\text{-4-(diethylphosphino)indene}$)] (7a). Prepared according to the general procedure from $[\text{Ru}(\eta^5\text{-Cp})(\eta^5\text{-4-bromindene})]$ ((\pm) -**3a**, 150 mg, 0.42 mmol), *t*BuLi (1.95 M, 431 μL , 0.84 mmol), and Et_2PCL (102 μL , 0.84 mmol) in diethyl ether (4.0 mL). A yellow solid was obtained after purification by flash chromatography (pentane, then pentane/ CH_2Cl_2 1/1) (85 mg, 55% yield). Mp: 38–40 °C. ^1H NMR (500 MHz, CD_2Cl_2): δ 7.37 (dd, $J = 8.6$, 0.7 Hz), 6.92 (td, $J = 6.4$, 0.9 Hz), 6.78 (dd, $J = 8.6$, 6.5 Hz), 5.45–5.44 (m, 1H), 5.23–5.22 (m, 1H), 4.64 (t, $J = 2.5$ Hz), 4.20 (s, 5H), 1.98–1.72 (m, 4H), 1.10–1.04 (m, 6H). ^{13}C NMR (125 MHz, CD_2Cl_2): δ 136.4 (d, $J = 19.2$ Hz), 127.6, 126.0 (d, $J = 6.0$ Hz), 122.7 (d, $J = 3.4$ Hz), 95.9 (d, $J = 21.8$ Hz), 92.0 (d, $J = 4.6$ Hz), 73.2, 70.4, 66.1 (d, $J = 9.6$ Hz), 66.0 (d, overlap), 18.6 (d, $J = 11.7$ Hz), 18.1 (d, $J = 11.2$ Hz), 10.4 (d, $J = 15.0$ Hz), 10.1 (d, $J = 12.2$ Hz). ^{31}P NMR (162 MHz, CDCl_3): $\delta -20.9$. HRMS (ESI) for $\text{C}_{18}\text{H}_{22}\text{PRu} [\text{M} + \text{H}]^+$: calcd 371.0497, found 371.0490.

[Fe($\eta^5\text{-Cp}^*$)($\eta^5\text{-4-(diphenylphosphino)indene}$)] (8b). Prepared according to the general procedure from $[\text{Fe}(\eta^5\text{-Cp}^*)(\eta^5\text{-4-bromindene})]$ ((\pm) -**4b**, 70.4 mg, 0.18 mmol), *t*BuLi (1.96 M, 190 μL , 0.37 mmol), and Ph_2PCL (50 μL , 0.28 mmol) in diethyl ether (2.0 mL). The reaction was quenched by the addition of brine. The aqueous phase was extracted with diethyl ether, dried over Na_2SO_4 , and concentrated. A purple solid was obtained after purification by flash chromatography (pentane, 1% Et_3N) (61.7, 68% yield). Mp: 158–161 °C (lit. 159–161 °C). ^1H NMR (500 MHz, C_6D_6): δ 7.62–7.57 (m, 2H), 7.42–7.36 (m, 2H), 7.21 (d, $J = 8.5$ Hz, 1H), 7.18–7.08 (m, 3H), 7.10–6.90 (m, 3H), 6.77–6.71 (m, 1H), 6.68 (t, $J = 5.8$ Hz, 1H), 4.46 (d, $J = 1.8$ Hz, 1H), 4.15 (t, $J < 1$ Hz, 1H), 3.57 (t, $J = 2.4$ Hz, 1H), 1.70 (s, 15H). ^{13}C NMR (125 MHz, C_6D_6): δ 137.2 (d, $J = 13.7$ Hz); 137.0 (d, $J = 10.9$ Hz), 137.0 (d, $J = 12.0$ Hz), 135.2 (d, $J = 20.2$ Hz), 134.4 (d, $J = 20.1$ Hz), 129.2, 128.8 (d, $J = 7.3$ Hz); 128.8, 128.8, 128.7 (d, $J = 7.1$ Hz), 127.4, 122.2, 91.2 (d, $J = 23.6$ Hz), 88.2 (d, $J = 6.0$ Hz), 78.1, 76.8, 66.7 (d, $J = 10.4$ Hz), 66.3 (d, $J = 1.9$ Hz), 10.4 (d, $J = 2.5$ Hz). ^{31}P NMR (202 MHz, CD_2Cl_2): $\delta -12.0$. IR: 3068, 3052, 2964, 2901, 2856, 1587, 1476, 1434, 1380, 1327, 1031, 910, 742, 696 cm^{-1} . HRMS (ESI) for $\text{C}_{31}\text{H}_{31}\text{FeP} [\text{M}, ^{56}\text{Fe}]^+$: calcd 490.150, found 490.1517.

Representative Procedure for the Microwave-Assisted Suzuki–Miyaura Cross-Coupling. The crystalline mixture of **2b** and over-reduced complex **18b** (90% **2b** (97% ee (*S*)) and 10% **18b**, 323.3 mg, 0.50 mmol of **2b**), $\text{Pd}(\text{OAc})_2$ (5.6 mg, 0.025 mmol, 5 mol %), *o*TolP (15.2 mg, 0.050 mmol, 10 mol %), $\text{PhB}(\text{OH})_2$ (**a**; 183 mg, 1.5 mmol), and K_3PO_4 (318 mg, 1.5 mmol) were placed in a 20 mL microwave vial, which was then sealed and purged with N_2 . Degassed methanol (12 mL) was added, and the mixture was sonicated for 2 min before being subjected to microwave irradiation for 15 min at 100 °C (prestirring 30 s; initial power ca. 180 W; after the temperature had reached 100 °C, the temperature was maintained for 15 min with a power of ca. 30 W). The mixture was filtered through Celite and washed with CH_2Cl_2 . After evaporation of the solvents, the residue was dissolved in CH_2Cl_2 (40 mL), washed with saturated NaHCO_3 (3 \times 30 mL) and then with water (2 \times 40 mL), and dried over MgSO_4 . The solvent was removed, and the residue was dissolved in acetone (10 mL). KPF_6 (386 mg, 2.1 mmol) was added, and the mixture was stirred at room temperature for 30 min. The solvent was removed, and the crude product was passed through a short column of neutral alumina. The enantiomeric purity of the coupled product was determined by ^1H NMR analysis with 1.7 equiv of $[\text{nBu}_4\text{N}][\Delta\text{-TRISPHAT}]$ using CDCl_3 as solvent.

[Ru($\eta^5\text{-Cp}^*$)($\eta^5\text{-5-phenylnaphthalene}$)](PF_6) (9ba). Purification through neutral alumina (CH_2Cl_2 , then CH_2Cl_2 /acetone 2:1) and crystallization from CH_2Cl_2 /diethyl ether gave complex **9ba** as orange crystals (155 mg, 53% yield, 99% ee (*S*)). Mp: 213–214 °C. $[\alpha]_D = +434^\circ$ ($c = 0.59$, CHCl_3). ^1H NMR (400 MHz, CDCl_3): δ 7.74–7.38 (m, 8H), 6.65 (d, $J = 6.0$ Hz, 1H), 6.41 (d, $J = 6.0$ Hz, 1H), 6.12 (t, $J = 6.0$ Hz, 1H), 6.00 (t, $J = 6.0$ Hz, 1H), 1.62 (s, 15H). ^{13}C NMR (100 MHz, CDCl_3): δ 139.8, 137.5, 131.1, 130.6, 129.7, 129.6, 129.3, 128.0, 97.9, 96.8, 94.6, 89.3, 88.6, 85.8, 83.4, 10.0. ^{31}P NMR (162 MHz,

CDCl₃): δ -143.8 (sept, J = 713 Hz). IR: 2922, 1475, 1450, 1387, 1354, 1078, 1031, 868, 831, 792, 760, 738, 705, 695, 617 cm⁻¹. HRMS (ESI) for C₂₆H₂₇Ru [M - PF₆]⁺: calcd 441.1150, found 441.1159. Anal. Calcd for C₂₆H₂₇PF₆Ru (585.53): C, 53.33; H, 4.65. Found: C, 53.10; H, 4.63.

[Ru(η^5 -Cp*)(η^6 -5-(*p*-methylphenyl)naphthalene)][PF₆] (9bb). Prepared according to the general procedure using the crystalline mixture of complexes **2b** and **18b** (90% **2b** (97% ee (S)) and 10% **18b**, 65 mg, 0.10 mmol of **2b**), Pd(OAc)₂ (1.1 mg, 0.005 mmol), *o*Tol₃P (3.04 mg, 0.010 mmol), *p*-MePhB(OH)₂ (**b**; 40.8 mg, 0.3 mmol), and K₃PO₄ (63.7 mg, 0.3 mmol) in methanol (2 mL). Purification through neutral alumina (CH₂Cl₂, then CH₂Cl₂/acetone 1/1) and crystallization from CH₂Cl₂/diethyl ether gave complex **9bb** as orange crystals (45 mg, 75% yield, 99% ee (S)). Mp: 194–195 °C. [α]_D = +452° (c = 0.1, CHCl₃). ¹H NMR (300 MHz, CDCl₃): δ 7.73–7.64 (m, 1H), 7.61–7.55 (m, 2H), 7.33 (q, J = 8.1 Hz, 4H), 6.63 (d, J = 6.0 Hz, 1H), 6.42 (d, J = 6.2 Hz, 1H), 6.11 (t, J = 5.9 Hz, 1H), 5.98 (t, J = 6.0 Hz, 1H), 2.46 (s, 3H), 1.62 (s, 15H). ¹³C NMR (75 MHz, CDCl₃): δ 139.5, 137.2, 135.6, 130.7, 129.4, 128.7, 127.6, 98.2, 97.0, 94.2, 89.3, 88.4, 85.8, 83.3, 21.5, 9.6. ³¹P NMR (162 MHz, CDCl₃): δ -143.8 (sept, J = 713 Hz). IR: 2919, 1615, 1509, 1474, 1387, 1074, 1031, 828, 739, 741, 674 cm⁻¹. HRMS (ESI) for C₂₇H₂₉Ru [M - PF₆]⁺: calcd 455.1307, found 455.1307.

[Ru(η^5 -Cp*)(η^6 -5-(*p*-methoxyphenyl)naphthalene)][PF₆] (9bc). Prepared according to the general procedure using the crystalline mixture of complexes **2b** and **18b** (90% **2b** (97% ee (S)) and 10% **18b**, 65 mg, 0.10 mmol of **2b**), Pd(OAc)₂ (1.1 mg, 0.005 mmol), *o*Tol₃P (3.04 mg, 0.010 mmol), *p*-MeOPhB(OH)₂ (**c**; 45.6 mg, 0.3 mmol), and K₃PO₄ (63.7 mg, 0.3 mmol) in methanol (2 mL). Purification through neutral alumina (CH₂Cl₂, then CH₂Cl₂/acetone 1/1) gave complex **9bc** as an orange solid (34 mg, 54% yield, 99% ee (S)). Mp: 196–197 °C. [α]_D = +461° (c = 0.1, CHCl₃). ¹H NMR (300 MHz, CDCl₃): δ 7.65 (dd, J = 8.5, 7.0 Hz, 1H), 7.57–7.46 (m, 2H), 7.33 (d, J = 8.6 Hz, 2H), 7.05 (d, J = 8.7 Hz, 2H), 6.57 (d, J = 5.9 Hz, 1H), 6.43 (d, J = 6.1 Hz, 1H), 6.05 (t, J = 5.8 Hz, 1H), 5.96 (t, J = 5.9 Hz, 1H), 3.87 (s, 3H), 1.58 (s, 15H). ¹³C NMR (75 MHz, CDCl₃): δ 160.2, 139.3, 130.6, 130.3, 129.3, 127.0, 114.7, 97.7, 96.6, 94.1, 89.0, 88.3, 85.5, 83.1, 55.5, 9.6. ³¹P NMR (162 MHz, CDCl₃): δ -143.8 (sept, J = 713 Hz). IR: 2921, 1607, 1508, 1472, 1387, 1248, 1179, 1028, 831, 742, 675 cm⁻¹. HRMS (ESI) for C₂₇H₂₉ORu [M - PF₆]⁺: calcd 471.1256, found 471.1238.

[Ru(η^5 -Cp*)(η^6 -5-(1-naphthyl)naphthalene)][PF₆] (9bd). Prepared according to the general procedure using the crystalline mixture of complexes **2b** and **18b** (90% **2b** (97% ee (S)) and 10% **18b**, 65 mg, 0.10 mmol of **2b**), Pd(OAc)₂ (1.1 mg, 0.005 mmol), *o*Tol₃P (3.04 mg, 0.010 mmol), 1-naphB(OH)₂ (**d**; 51.6 mg, 0.3 mmol), and K₃PO₄ (63.7 mg, 0.3 mmol) in methanol (2 mL). Purification through neutral alumina (CH₂Cl₂, then CH₂Cl₂/acetone 1/1) and crystallization from CH₂Cl₂/diethyl ether gave complex **9bd** as orange crystals (23 mg, 50% yield, 99% ee (S)). Mp: 230–233 °C. [α]_D = +425° (c = 0.1, CHCl₃). ¹H NMR (300 MHz, CDCl₃): δ 8.03 (d, J = 8.2 Hz, 1H), 7.97 (d, J = 8.2 Hz, 1H), 7.82–7.69 (m, 3H), 7.64 (t, J = 7.6 Hz, 1H), 7.53 (t, J = 7.5 Hz, 1H), 7.46 (d, J = 6.8 Hz, 1H), 7.34 (t, J = 7.7 Hz, 1H), 7.09 (d, J = 8.6 Hz, 1H), 6.76 (d, J = 6.0 Hz, 1H), 6.12 (t, J = 6.2 Hz, 1H), 5.72 (m, 2H), 1.67 (s, 15H). ¹³C NMR (75 MHz, CDCl₃): δ 138.3, 134.8, 133.7, 132.1, 130.9, 130.5, 130.0, 128.9, 128.3, 127.2, 127.2, 126.7, 125.5, 125.3, 98.9, 96.0, 94.3, 89.0, 88.2, 85.5, 83.6, 9.8. ³¹P NMR (162 MHz, CDCl₃): δ -143.8 (sept, J = 713 Hz). IR: 3087, 3042, 1666, 1405, 1333, 1245, 1098, 1026, 996, 809, 744, 724 cm⁻¹. HRMS (ESI) for C₃₀H₂₉Ru [M - PF₆]⁺: calcd 491.1307, found 491.1308.

[Ru(η^5 -Cp*)(η^6 -5-(*E*)-2-cyclohexylvinyl)naphthalene)][PF₆] (9be). Prepared according to the general procedure using the crystalline mixture of complexes **2b** and **18b** (85% **2b** (97% ee (S)) and 15% **18b**, 338.1 mg, 0.50 mmol of **2b**), Pd(OAc)₂ (5.6 mg, 0.025 mmol), *o*Tol₃P (15.2 mg, 0.050 mmol), (*E*)-2-cyclohexylvinylboronic acid (**e**; 231.0 mg, 1.5 mmol), and K₃PO₄ (318 mg, 1.5 mmol) in methanol (12 mL). Purification through neutral alumina (CH₂Cl₂, then CH₂Cl₂/acetone 2/1) and crystallization from CH₂Cl₂/diethyl ether gave complex **9be** as yellow crystals (225 mg, 73% yield, 99% ee

(S)). Mp: 207–208 °C. [α]_D = +474° (c = 0.63, CHCl₃). ¹H NMR (400 MHz, CDCl₃): δ 7.51–7.66 (m, 2H), 7.38 (d, 1H, J = 8.6 Hz), 6.67 (d, 1H, J = 15.7 Hz), 6.56–6.62 (m, 1H), 6.44–6.52 (m, 1H), 6.21 (dd, 1H, J = 15.7, 7.3 Hz), 5.98–6.11 (m, 2H), 2.22–2.34 (m, 1H), 1.63 (s, 15H), 1.14–1.91 (m, 10H). ¹³C NMR (100 MHz, CDCl₃): δ 144.4, 137.0, 131.1, 126.7, 126.5, 122.4, 97.3, 95.9, 94.4, 89.0, 88.6, 85.9, 81.9, 41.9, 33.1, 26.3, 26.2, 9.9. ³¹P NMR (162 MHz, CDCl₃): δ -143.8 (sept, J = 713 Hz). IR: 3097, 2923, 2851, 1641, 1612, 1475, 1449, 1388, 1074, 1030, 968, 872, 825, 741 cm⁻¹. HRMS (ESI) for C₂₈H₃₅Ru [M - PF₆]⁺: calcd 473.1776, found 473.1749.

Representative Procedure for the Microwave-Assisted C–P Cross-Coupling. The crystalline mixture of **2b** and over-reduced complex **18b** (79% **2b** (99% ee (S)) and 21% **18b**, 363.2 mg, 0.50 mmol of **2b**), Pd(dba)₂ (8.6 mg, 0.015 mmol, 3 mol %), ddpf (8.3 mg, 0.015 mmol, 3 mol %), and K₃PO₄ (180 mg, 0.85 mmol) were placed in a microwave vial, which was then sealed and purged with N₂. Dry, degassed CH₂Cl₂ (1.5 mL) was added, and the mixture was stirred for a few minutes before diphenylphosphine (0.148 mL, 0.85 mmol) was added. The mixture was sonicated for 2 min before being subjected to microwave irradiation for 40 min at 105 °C (preirradiation 30 s; initial power ca. 75 W; after the temperature had reached 105 °C, the temperature was maintained for 40 min with a power of ca. 20 W). The crude product was purified by column chromatography on silica gel. The enantiomeric purity of the phosphine was determined by ¹H NMR and ³¹P NMR (CDCl₃) after coordination to a chiral palladium template (2 equiv).⁵⁰

[Ru(η^5 -Cp*)(η^6 -5-(diphenylphosphino)naphthalene)][PF₆] (10b). Purification through two successive flash chromatographies (CH₂Cl₂, then CH₂Cl₂/acetone 5/1) afforded phosphine **10b** as a yellow solid (252 mg, 73% yield, 99% ee (S)). Mp: 107–109 °C. [α]_D = +485° (c = 0.62, CHCl₃). ¹H NMR (400 MHz, CDCl₃): δ 7.21–7.61 (m, 12H), 6.97–7.04 (m, 1H), 6.64 (d, ³ J = 5.8 Hz, 1H), 5.54–6.61 (m, 1H), 6.11 (t, J = 5.8 Hz, 1H), 5.84 (t, J = 5.8 Hz, 1H), 1.74 (s, 15H). ¹³C NMR (100 MHz, CDCl₃): δ 137.4 (d, J = 20.2 Hz), 135.7, 134.9 (d, J = 20.2 Hz), 134.4 (d, J = 20.2 Hz), 133.6 (d, J = 6.4 Hz), 133.2 (d, J = 8.3 Hz), 130.5, 130.3, 130.1, 129.7 (d, J = 8.3 Hz), 129.5 (d, J = 7.4 Hz), 129.2, 98.5 (d, J = 21.1 Hz), 97.0 (d, J = 2.8 Hz), 94.7, 89.1, 88.2, 86.3, 83.2 (d, J = 25.7 Hz), 10.0 (d, J = 1.8 Hz). ³¹P NMR (162 MHz, CDCl₃): δ -13.3, -144.1 (sept, J = 713 Hz). IR: 2913, 1474, 1435, 1387, 1340, 1074, 1029, 913, 830, 735, 696, 665 cm⁻¹. HRMS (ESI) for C₃₂H₃₂PRu [M - PF₆]⁺: calcd 549.1279, found 549.1299. Anal. Calcd for C₃₂H₃₂P₂F₆Ru·0.5CH₂Cl₂ (736.07): C, 53.03; H, 4.52. Found: C, 53.15; H, 4.21.

[Ru(η^5 -Cp*)(η^6 -5-(diphenylphosphino)naphthalene)][PF₆] (10a). Prepared according to the general procedure from (\pm)-**2a** (52 mg, 0.1 mmol), Pd(dba)₂ (2.9 mg, 0.005 mmol), ddpf (2.8 mg, 0.005 mmol), K₃PO₄ (31.8 mg, 0.15 mmol), and diphenylphosphine (26 μ L, 0.15 mmol) in CH₂Cl₂ (1 mL). The microwave irradiation time was reduced to 5 min. Purification through flash chromatography (CH₂Cl₂, then CH₂Cl₂/acetone 6/1) afforded phosphine **10a** as a yellow solid (28 mg, 45% yield). Mp: 159–161 °C. ¹H NMR (500 MHz, CD₂Cl₂): δ 7.72 (d, J = 8.5 Hz, 1H), 7.47–7.54 (m, 6H), 7.38–7.43 (m, 3H), 7.26–7.33 (m, 4H), 6.96 (d, J = 6.0 Hz, 1H), 6.28 (t, J = 6.0 Hz, 1H), 6.15 (t, J = 5.7 Hz, 1H), 4.78 (s, 5H). ¹³C NMR (125 MHz, CD₂Cl₂): δ 139.3 (d, J = 22.0 Hz), 137.6, 135.3 (d, J = 21.5 Hz), 134.0 (d, J = 8.3 Hz), 134.0 (d, J = 19.7 Hz), 133.1 (d, J = 8.8 Hz), 131.5, 131.1, 130.6, 130.1, 129.6 (d, J = 8.3 Hz), 129.5 (d, J = 7.3 Hz), 99.6 (d, J = 25.2 Hz), 97.5 (d, J = 3.7 Hz), 86.2, 85.8 (d, J = 1.8 Hz), 84.9, 82.2 (d, J = 29.3 Hz), 80.2. ³¹P NMR (202 MHz, CD₂Cl₂): δ -16.5, -144.1 (sept, J = 711 Hz). IR: 3117, 1607, 1477, 1435, 1341, 1195, 824, 792, 748, 736, 697, 665 cm⁻¹. HRMS (ESI) for C₂₇H₂₂PRu [M - PF₆]⁺: calcd 479.0502, found 479.0491. Anal. Calcd for C₂₇H₂₂P₂F₆Ru·0.15CH₂Cl₂ (636.21): C, 51.26; H, 3.53. Found: C, 51.25; H, 3.32.

[Ru(η^5 -Cp*)(η^6 -5-(bis(3,5-dimethylphenyl)phosphino)naphthalene)][PF₆] (11b). Prepared according to the general procedure from (\pm)-**2b** (69.3 mg, 0.118 mmol), Pd(dba)₂ (3.4 mg, 0.006 mmol, 5 mol %), ddpf (3.4 mg, 0.006 mmol, 5 mol %), K₃PO₄ (50.3 mg, 0.240 mmol), and bis(3,5-dimethylphenyl)phosphine (65.0 mg, 0.19 mmol) in CH₂Cl₂ (1.2 mL). Purification through flash

chromatography (CH₂Cl₂, then CH₂Cl₂/acetone 20/1) and recrystallization from Et₂O/CH₂Cl₂ at 4 °C afforded phosphine **11b** as yellow plates (69 mg, 77% yield). Mp: >240 °C dec. ¹H NMR (500 MHz, CD₂Cl₂): δ 7.51 (ddd, *J* = 8.7, 6.7, <1 Hz, 1H), 7.46 (br d, *J* = 8.7 Hz, 1H), 7.13 (br s, 1H), 7.10 (ddd, *J* = 6.7, 3.6, 1.2 Hz, 1H), 7.03 (br s, 1H), 6.96 (br d, *J* = 9.0 Hz, 1H), 6.89 (br d, *J* = 8.7 Hz, 1H), 6.65–6.61 (m, 1H), 6.42 (d, *J* = 6.0 Hz, 1H), 5.95 (t, *J* = 5.8 Hz, 1H), 5.76 (td, *J* = 6.0, <1 Hz, 1H), 2.31 (s, 6H), 2.21 (s, 6H), 1.73 (s, 15H). ¹³C NMR (125 MHz, CD₂Cl₂): δ 139.3 (d, *J* = 8.4 Hz, 1C), 139.1 (d, *J* = 8.4 Hz), 138.4 (d, *J* = 20.7 Hz), 136.1 (d, *J* = 1.5 Hz), 133.6 (d, *J* = 6.2 Hz), 133.0 (d, *J* = 7.9 Hz), 132.7 (d, *J* = 21.2 Hz), 132.3, 132.1 (d, *J* = 20.9 Hz), 132.0, 130.7, 128.3, 98.8 (d, *J* = 20.6 Hz), 97.3 (d, *J* = 3.1 Hz), 94.7, 88.6 (d, *J* = 1.3 Hz), 87.0 (d, *J* = 1.5 Hz), 86.0 (d, *J* = 1.4 Hz), 83.6 (d, *J* = 26.0 Hz), 21.4, 21.3, 10.0 (d, *J* = 2.0 Hz). ³¹P NMR (202 MHz, CD₂Cl₂): δ -13.2, -144.4 (sept, *J* = 711 Hz). IR: 3091, 2915, 2860, 1600, 1472, 1456, 1387, 1344, 1183, 1224, 1034, 874, 829, 791, 692 cm⁻¹. HRMS (ESI) for C₃₆H₄₀PRu [M - PF₆⁻, ¹⁰²Ru]⁺: calcd 605.1905, found 605.1878. Anal. Calcd for C₃₆H₄₀F₆P₂Ru·0.9CH₂Cl₂ (826.2): C, 53.65; H, 5.10. Found: C, 53.67; H, 5.06.

[Ru(η⁵-Cp*)(η⁶-5-(*di*-*o*-tolylphosphino)naphthalene)][PF₆]⁻ (**12b**). Prepared according to the general procedure using the crystalline mixture of complexes **2b** and **18b** (85% **2b** (97% ee (*S*)) and 15% **18b**, 57.4 mg, 0.085 mmol of **2b**), Pd(dba)₂ (4.9 mg, 0.0085 mmol, 10 mol %), ddpf (3.5 mg, 0.0085 mmol, 10 mol %), K₃PO₄ (28.4 mg, 0.134 mmol), and *di*-*o*-tolylphosphine (32.8 mg, 0.138 mmol) in CH₂Cl₂ (1.2 mL). The reaction mixture was subjected to 1 h of microwave irradiation at 140 °C. Purification through flash chromatography (CH₂Cl₂, then CH₂Cl₂/acetone 20/1) and recrystallization from Et₂O/CH₂Cl₂ at 4 °C afforded phosphine **12b** as yellow plates (24.7 mg, 40% yield, 99% ee (*S*)). Mp: 142–144 °C. [α]_D²⁰ = +554° (*c* = 0.87, CHCl₃). ¹H NMR (500 MHz, CD₂Cl₂): δ 7.53–7.45 (m, 2H), 7.43–7.36 (m, 2H), 7.31–7.23 (m, 2H), 7.20–7.14 (m, 1H), 7.07–7.03 (m, 1H), 7.00–6.94 (m, 1H), 6.90–6.84 (m, 1H), 6.59–6.54 (m, 1H), 6.48 (ddd, *J* = 6.2, 4.1, <1 Hz, 1H), 6.41 (d, *J* = 6.0 Hz, 1H), 5.92 (td, *J* = 5.7, <1 Hz, 1H), 5.74–5.69 (m, 1H), 2.66 (s, 3H), 2.42 (d, *J* = 1.3 Hz, 3H), 1.73 (s, 15H). ¹³C NMR (125 MHz, CD₂Cl₂): δ 144.3 (d, *J* = 28.5 Hz), 142.9 (d, *J* = 28.2 Hz), 136.8 (d, *J* = 21.0 Hz), 136.3 (d, *J* = 3.5 Hz), 135.2, 134.0, 133.5 (d, *J* = 6.8 Hz), 131.2 (d, *J* = 5.5 Hz), 130.9 (d, *J* = 8.0 Hz), 130.9 (d, *J* = 5.9 Hz), 130.8, 130.8, 130.1, 128.4 (d, *J* = 1.4 Hz), 127.5 (d, *J* = 1.4 Hz), 126.7, 100.0 (d, *J* = 19.4 Hz), 96.9 (d, *J* = 2.7 Hz), 95.0, 88.7 (d, *J* < 1 Hz), 87.8 (d, *J* = 1.4 Hz), 85.7 (d, *J* < 1 Hz), 83.8 (d, *J* = 23.3 Hz), 21.9 (d, *J* = 22.0 Hz), 21.0 (d, *J* = 22.9 Hz), 10.1 (d, *J* = 1.1 Hz). ³¹P NMR (202 MHz, CD₂Cl₂): δ -27.6, -144.1 (sept, *J* = 711 Hz). IR: 2965, 2916, 2860, 1470, 1454, 1384, 1033, 874, 830, 754 cm⁻¹. HRMS (ESI) for C₃₄H₃₆PRu [M - PF₆⁻, ¹⁰²Ru]⁺: calcd 577.1564, found 577.1598. Anal. Calcd for C₃₄H₃₆F₆P₂Ru·CH₂Cl₂ (806.6): C, 52.12; H, 4.75. Found: C, 52.25; H, 4.58.

[Ru(η⁵-Cp*)(η⁶-5-(*diphenylphosphino*)naphthalene)][BAR^F]⁻ (**10b**). (±)-[**10b**][BAR^F]⁻ (131.50 mg, 0.223 mmol) and NaBAR^F (200.00 mg, 0.226 mmol) were charged in a Schlenk tube. Dry and degassed CH₂Cl₂ (26 mL) was added, and the resulting cloudy yellow solution was stirred for 15 min at room temperature. The solvent was evaporated to dryness. The residue was redissolved in dry CH₂Cl₂ (6 mL), filtered, and washed (12 mL). The filtrate was concentrated to afford (±)-[**10b**][BAR^F]⁻ as a yellow solid (279 mg, 96% yield). ¹H NMR (500 MHz, CD₂Cl₂): δ 7.74 (s, 8H), 7.57 (s, 4H), 7.52–7.45 (m, 4H), 7.43–7.39 (m, 1H), 7.37–7.27 (m, 7H), 7.10 (ddd, *J* = 6.8, 3.5, 1.0 Hz, 1H), 6.68 (dd, *J* = 5.5, <1 Hz, 1H), 6.23 (d, *J* = 6.0 Hz, 1H), 5.78 (t, *J* = 5.8 Hz, 1H), 5.70 (t, *J* = 6.0 Hz, 1H), 1.70 (s, 15H). ¹³C NMR (125 MHz, CD₂Cl₂): δ 162.3 (q, ¹J_{C,B} = 49.9 Hz, C_{ipsoBAR^F}), 138.3 (d, *J* = 20.8 Hz), 136.5 (d, *J* = 1.5 Hz), 135.3 (br s, C_{orthoBAR^F}), 135.1, 134.6 (d, *J* = 20.6 Hz), 133.8 (d, *J* = 6.8 Hz), 133.1 (d, *J* = 8.2 Hz), 131.1, 130.9, 130.6, 129.9 (d, *J* = 7.9 Hz), 129.7 (d, *J* = 8.0 Hz), 129.4 (qq, ²J_{C,F} = 31.5, ³J_{C,B} = 2.9 Hz, CCF₃), 128.1, 125.1 (q, ¹J_{C,F} = 272.4 Hz, CF₃), 118.0 (br s, C_{paraBAR^F}), 99.0 (d, *J* = 20.6 Hz), 97.3 (d, *J* = 3.1 Hz), 95.2, 88.3, 87.8 (d, *J* = 1.6 Hz), 85.7, 83.7 (d, *J* = 26.3 Hz), 10.2 (d, *J* = 1.9 Hz). ³¹P NMR (162 MHz, CD₂Cl₂): δ -13.1. IR: 2963, 1610, 1475, 1437, 1353, 1272, 1115, 1028, 886, 838, 744, 696, 712, 669, 681 cm⁻¹. HRMS (ESI) for C₃₂H₃₂PRu [M - BAR^F]⁺: calcd

549.1279, found 549.1254. Anal. Calcd for C₆₄H₄₄PBF₂₄Ru (1411.85): C, 54.45; H, 3.14. Found: C, 54.74; H, 3.45.

Representative Procedure for the Synthesis of Gold(I) Complexes. AuCl·SMe₂ (34.0 mg, 0.115 mmol) was added to a solution of **10b** (80.0 mg, 0.115 mmol, 99% ee (*S*)) in CH₂Cl₂ (1.0 mL) followed by CH₂Cl₂ (1.0 mL) at ambient temperature in the dark. After 4 h (the initially intense yellow color almost vanished), the reaction mixture was filtered over a pad of Celite, which was washed with CH₂Cl₂, and the eluent was concentrated. This procedure was repeated several times until the product became pale yellow and no black precipitate was observed.

[AuCl((*S*)-**10b**)] ((*S*)-**13b**). A yellow solid was obtained after precipitation in pentane (61.4 mg, quantitative). Yellow crystals suitable for X-ray analysis were grown by slow diffusion of Et₂O in a CH₂Cl₂ solution of (*S*)-**13** at 4 °C. Mp: 210 °C dec. [α]_D²⁰ = +305.6° (*c* = 1.01, CH₂Cl₂). ¹H NMR (500 MHz, CD₂Cl₂): δ 7.83 (d, *J* = 8.7 Hz, 1H), 7.72–7.67 (m, 1H), 7.67–7.55 (m, 6H), 7.50–7.40 (m, 4H), 7.27–7.21 (m, 2H), 6.53 (d, *J* = 6.0 Hz, 1H), 6.01 (td, *J* = 6.0, <1 Hz, 1H), 5.85–5.82 (m, 1H), 1.81 (s, 15H). ¹³C NMR (125 MHz, CD₂Cl₂): δ 140.1 (d, *J* = 5.9 Hz), 135.4 (d, *J* = 14.4 Hz), 135.3 (d, *J* = 14.5 Hz), 134.7 (d, *J* = 2.4 Hz), 133.6 (d, *J* = 2.7 Hz), 133.6 (d, *J* = 2.6 Hz), 130.4 (d, *J* = 12.4 Hz), 130.2 (d, *J* = 12.4 Hz), 129.2 (d, *J* = 10.6 Hz), 126.4 (d, *J* = 19.5 Hz), 126.1 (d, *J* = 14.3 Hz), 125.7 (d, *J* = 22.8 Hz), 99.0 (d, *J* = 11.9 Hz), 96.2, 95.4 (d, *J* = 6.1 Hz), 89.0, 87.6, 86.3 (d, *J* < 1 Hz), 83.2 (d, *J* = 14.4 Hz), 10.7. ³¹P NMR (202 MHz, CD₂Cl₂): δ +24.4, -144.3 (sept, *J* = 711 Hz). IR: 3062, 2912, 1611, 1473, 1438, 1387, 1268, 1100, 1028, 831, 729, 692 cm⁻¹. HRMS (ESI) for C₃₂H₃₂ClPRuAu [M - PF₆⁻, ³⁵Cl, ¹⁰²Ru, ¹⁹⁷Au]⁺: calcd 781.0633, found 781.0640. Anal. Calcd for C₃₂H₃₂AuClF₆P₂Ru·0.6CH₂Cl₂ (977.0): C, 40.08; H, 3.43. Found: C, 40.10; H, 3.30.

[AuCl(**11b**)] (**14b**). Prepared according to the general procedure from (±)-**11b** (30.7 mg, 0.041 mmol) and AuCl·SMe₂ (13.3 mg, 0.045 mmol). A yellow solid was obtained after precipitation in pentane (44.1 mg, quantitative). Yellow crystals suitable for X-ray analysis were grown by slow diffusion of Et₂O in a CH₂Cl₂ solution of **14** at 4 °C. Mp: >215 °C dec. ¹H NMR (500 MHz, CD₂Cl₂): δ 7.81 (d, *J* = 8.6 Hz, 1H), 7.64 (ddd, *J* = 8.5, 7.0, 1.3 Hz, 1H), 7.30 (br s, 1H), 7.24 (dd, *J* = 11.8, 6.7 Hz, 1H), 7.23 (d, *J* = 6.5 Hz, 1H), 7.18 (br s, 1H), 7.17 (d, *J* = 14.8 Hz, 2H), 6.99 (d, *J* = 14.3 Hz, 2H), 6.53 (d, *J* = 5.8 Hz, 1H), 5.99 (t, *J* = 5.8 Hz, 1H), 5.81 (t, *J* = 6.0 Hz, 1H), 2.37 (s, 6H), 2.23 (s, 6H), 1.81 (s, 15H). ¹³C NMR (125 MHz, CD₂Cl₂): δ 140.5 (d, *J* = 13.0 Hz), 140.2 (d, *J* = 13.1 Hz), 140.0 (d, *J* = 6.0 Hz), 135.3 (d, *J* = 2.8 Hz), 135.3 (d, *J* = 2.5 Hz), 134.4 (d, *J* = 2.4 Hz), 132.8 (d, *J* = 14.4 Hz), 132.5 (d, *J* = 14.5 Hz), 129.3 (d, *J* = 10.7 Hz), 126.9 (d, *J* = 55.8 Hz), 125.9 (d, *J* = 19.6 Hz), 125.4 (d, *J* = 19.7 Hz), 99.3 (d, *J* = 11.7 Hz), 96.1, 95.2 (d, *J* = 6.0 Hz), 88.8, 87.5, 86.2, 83.3 (d, *J* = 14.0 Hz), 21.5, 21.4, 10.7. ³¹P NMR (202 MHz, CD₂Cl₂): δ +24.4, -144.3 (sept, *J* = 711 Hz). IR: 2953, 2916, 2860, 1601, 1470, 1448, 1386, 1345, 1129, 1036, 832, 786, 731, 686 cm⁻¹. HRMS (ESI) for C₃₆H₄₀ClPRuAu [M - PF₆⁻, ¹⁰²Ru]⁺: calcd 837.1259, found 837.1271. Anal. Calcd for C₃₆H₄₀AuClF₆P₂Ru·(CH₂Cl₂)_{0.5} (1024.6): C, 42.79; H, 4.03. Found: C, 42.57; H, 3.58.

[AuCl(**12b**)] (**15b**). Prepared according to the general procedure from **12b** (11.7 mg, 0.016 mmol, 99% ee (*S*)) and AuCl·SMe₂ (5.0 mg, 0.017 mmol). A yellow solid was obtained after precipitation in pentane (19.0 mg, quant.). Mp: >200 °C dec. [α]_D²⁰ = +232° (*c* = 0.95, CH₂Cl₂). ¹H NMR (500 MHz, CD₂Cl₂): δ 7.89 (d, *J* = 8.7 Hz, 1H), 7.85–7.20 (m, 10H), 7.10–6.93 (m, 1H), 6.57 (d, 6.0 Hz, 1H), 6.04 (t, *J* = 5.9 Hz, 1H), 5.88 (d, *J* = 6.0 Hz, 1H), 3.10–2.50 (2 br s, 6H), 1.84 (s, 15H). ³¹P NMR (202 MHz, CD₂Cl₂): δ -3.1 (br), -144.1 (sept, *J* = 711 Hz). IR: 2961, 2910, 1608, 1589, 1472, 1450, 1381, 1260, 1071, 1025, 830, 818, 806, 768, 747 cm⁻¹. HRMS (ESI) for C₃₄H₃₆ClPRuAu [M - PF₆⁻, ¹⁰²Ru]⁺: calcd 809.0952, found 809.0850.

IR Spectroscopic Characterization of Phosphines. Ni(CO)₂L complexes were generated in situ from Ni(cod)₂ and carbon monoxide in CH₂Cl₂. The phosphine complexes were not isolated but directly analyzed in solution by means of FT-IR spectroscopy. **Caution!** Carbon monoxide is toxic; Ni(CO)₄ is very toxic and highly volatile. All transformations have to be carried out in a well-ventilated fume

hood, including the generation of Ni(CO)₄, preparation of IR samples, and cleanup. The waste can be destroyed by oxidation with bromine. Ni(cod)₂ is air-sensitive and rapidly decomposes to black Ni(0). All reactions were carried out with dry and degassed CH₂Cl₂. The IR cell was purged with nitrogen before use.

Ni(CO)₂L. Carbon monoxide was bubbled for 2–5 min through a yellow solution of Ni(cod)₂ (9.1–13.2 mg, 0.033–0.05 mmol) in CH₂Cl₂ (1.0 mL) until the yellow color vanished.⁵¹ A stock solution of the phosphine (ca. 0.1 M, 1.0 equiv) was added to the colorless clear solution of Ni(CO)₄, and the mixture was stirred for 5 min, followed by bubbling nitrogen through the solution for 5 min.⁵² IR spectra (2150–1850 cm⁻¹) were measured in transmission mode in a NaCl cuvette with a resolution of 1 cm⁻¹. The recorded ν_{CO(A₁)} values were referenced to the Tolman scale using ν_{CO(A₁)} of Ni(CO)₃(PPh₃) as a reference (lit.³² 2068.9 cm⁻¹, exptl 2069.5 cm⁻¹). The corrected values for ν_{CO(A₁)} are depicted in Table 3.

■ ASSOCIATED CONTENT

● Supporting Information

Text giving additional details about the crystal structures of **11b** and **12b**, tables and spectra giving NMR data, and CIF files giving X-ray crystallographic data for complexes **11b–14b** and **16b**. This material is available free of charge via the Internet at <http://pubs.acs.org>.

■ AUTHOR INFORMATION

Corresponding Author

*E-mail: peter.kundig@unige.ch.

■ ACKNOWLEDGMENTS

We thank the Swiss National Science Foundation and the University of Geneva for financial support.

■ REFERENCES

- (1) *Phosphorus Ligands in Asymmetric Catalysis: Synthesis and Applications*; Börner, A., Ed.; Wiley-VCH: Weinheim, Germany, 2008, Vol 1–3.
- (2) (a) *Ferrocenes*; Hayashi, T.; Togni, A., Eds.; Wiley-VCH: Weinheim, Germany, 1995. (b) Richards, C. J.; Locke, A. J. *Tetrahedron: Asymmetry* **1998**, *9*, 2377–2407. (c) Colacot, T. J. *Chem. Rev.* **2003**, *103*, 3101–3118. (d) Dai, L. X.; Tu, T.; You, S. L.; Deng, W. P.; Hou, X. L. *Acc. Chem. Res.* **2003**, *36*, 659–667. (e) Atkinson, R. C. J.; Gibson, V. C.; Long, N. J. *Chem. Soc. Rev.* **2004**, *33*, 313–328. (f) Siemeling, U.; Auch, T. C. *Chem. Soc. Rev.* **2005**, *34*, 584–594. (g) Arrayas, R. G.; Adrio, J.; Carretero, J. C. *Angew. Chem., Int. Ed.* **2006**, *45*, 7674–7715. (h) Fu, G. C. *Acc. Chem. Res.* **2006**, *39*, 853–860. (i) *Chiral Ferrocenes in Asymmetric Catalysis: Synthesis and Applications*; Dai, L. X., Hou, X. L., Eds.; Wiley-VCH: Weinheim, Germany, 2010.
- (3) (a) Muñoz, K.; Bolm, C. *Chem. Eur. J.* **2000**, *6*, 2309–2316. (b) You, S. L.; Hou, X. L.; Dai, L. X.; Yu, Y. H.; Xia, W. *J. Org. Chem.* **2002**, *67*, 4684–4695.
- (4) (a) Mancheno, O. G.; Priego, J.; Cabrera, S.; Arrayas, R. G.; Llamas, T.; Carretero, J. C. *J. Org. Chem.* **2003**, *68*, 3679–3686. (b) Thimmaiah, M.; Luck, R. L.; Fang, S. Y. *J. Organomet. Chem.* **2007**, *692*, 1956–1962.
- (5) (a) Bolm, C.; Muñoz, K. *Chem. Soc. Rev.* **1999**, *28*, 51–59. (b) Gibson, S. E.; Ibrahim, H. *Chem. Commun.* **2002**, 2465–2473. (c) Salzer, A. *Coord. Chem. Rev.* **2003**, *242*, 59–72. (d) Muñoz, K. In *Transition Metal Arene π-Complexes in Organic Synthesis and Catalysis*; Kundig, E. P., Ed.; Springer Verlag: Berlin, 2004; Topics in Organometallic Chemistry Vol. 7, p 205. (e) Rosillo, M.; Dominguez, G.; Perez-Castells, J. *Chem. Soc. Rev.* **2007**, *36*, 1589–1604.
- (6) For studies comparing ferrocene- and ruthenocene-derived ligands, see: (a) Hayashi, T.; Ohno, A.; Lu, S. J.; Matsumoto, Y.; Fukuyo, E.; Yanagi, K. *J. Am. Chem. Soc.* **1994**, *116*, 4221–4226. (b) Abbenhuis, H. C. L.; Burckhardt, U.; Gramlich, V.; Martelletti, A.; Spencer, J.; Steiner, I.; Togni, A. *Organometallics* **1996**, *15*, 1614–1621. (c) Garrett, C. E.; Fu, G. C. *J. Am. Chem. Soc.* **1998**, *120*, 7479–7483. (d) Bolm, C.; Hermanns, N.; Kesselgruber, M.; Hildebrand, J. P. *J. Organomet. Chem.* **2001**, *624*, 157–161. (e) Bäckvall, J. E.; Cotton, H. K.; Norinder, J. *Tetrahedron* **2006**, *62*, 5632–5640. (f) Carmichael, D.; Goldet, G.; Klankermayer, J.; Ricard, L.; Seeboth, N.; Stankevici, M. *Chem. Eur. J.* **2007**, *13*, 5492–5502. (g) Xie, F.; Liu, D. L.; Zhang, W. B. *Tetrahedron Lett.* **2008**, *49*, 1012–1015.
- (7) (a) Kundig, E. P.; Chaudhuri, P. D.; House, D.; Bernardinelli, G. *Angew. Chem., Int. Ed.* **2006**, *45*, 1092–1095. (b) Mercier, A.; Yeo, W. C.; Chou, J.; Chaudhuri, P. D.; Bernardinelli, G.; Kundig, E. P. *Chem. Commun.* **2009**, 5227–5229. (c) Mercier, A.; Urbaneja, X.; Yeo, W. C.; Chaudhuri, P. D.; Cumming, G. R.; House, D.; Bernardinelli, G.; Kundig, E. P. *Chem. Eur. J.* **2010**, *16*, 6285–6299. (d) Mercier, A.; Yeo, W. C.; Urbaneja, X.; Kundig, E. P. *Chimia* **2010**, *64*, 177–179.
- (8) Urbaneja, X.; Mercier, A.; Besnard, C.; Kundig, E. P. *Chem. Commun.* **2011**, *47*, 3739–3741.
- (9) Cumming, G. R.; Bernardinelli, G.; Kundig, E. P. *Chem. Asian J.* **2006**, *1*, 459–468.
- (10) A similar sequence was previously reported for the synthesis of analogue iron complex **8b**.^{4b}
- (11) The bromine/lithium exchange did not occur, as indicated by the formation of Ph₂(nBu)P (³¹P NMR (162 MHz, CD₂Cl₂): δ +16.5 ppm).
- (12) (a) Robertson, D. R.; Stephenson, T. A. *J. Organomet. Chem.* **1977**, *142*, C31–C34. (b) Volkenau, N. A.; Bolesova, I. N.; Shulpina, L. S.; Kitaigorodskii, A. N. *J. Organomet. Chem.* **1984**, *267*, 313–321. (c) Older, C. M.; Stryker, J. M. *J. Am. Chem. Soc.* **2000**, *122*, 2784–2797.
- (13) For addition of carbanions to cationic [Fe(η⁵-Cp)(η⁶-naphthalene)] complexes, see: (a) Nesmeyanov, A. N.; Solodovnikov, S. P.; Vol'kenau, N. A.; Kotova, L. S.; Sinitzyna, N. A. *J. Organomet. Chem.* **1978**, *148*, C5–C8. (b) Kundig, E. P.; Jeger, P.; Bernardinelli, G. *Angew. Chem., Int. Ed.* **1995**, *34*, 2161–2163.
- (14) For reviews on transition-metal-catalyzed C–P cross-coupling reactions, see: (a) Tappe, F. M. J.; Trepohl, V. T.; Oestreich, M. *Synthesis* **2010**, 3037–3062. (b) Glueck, D. S. In *C–X Bond Formation*; Vigalok, A., Ed.; Springer-Verlag: Berlin, 2010; Topics in Organometallic Chemistry Vol. 31, p 65.
- (15) For a review on Pd-catalyzed C–P bond formation processes, see: (a) Schwan, A. L. *Chem. Soc. Rev.* **2004**, *33*, 218–224. For a seminal paper, see: (b) Herd, O.; Hessler, A.; Hingst, M.; Tepper, M.; Stelzer, O. *J. Organomet. Chem.* **1996**, *522*, 69–76. For the use of secondary phosphines at room temperature, see: (c) Korff, C.; Helmchen, G. *Chem. Commun.* **2004**, 530–531. (d) Blank, N. F.; Moncarz, J. R.; Brunker, T. J.; Scriban, C.; Anderson, B. J.; Amir, O.; Glueck, D. S.; Zakharov, L. N.; Golen, J. A.; Incarvito, C. D.; Rheingold, A. L. *J. Am. Chem. Soc.* **2007**, *129*, 6847–6858. Selected examples for the use of secondary phosphine-boranes at room temperature: (e) Al-Masum, M.; Kumaraswamy, G.; Livinghouse, T. J. *Org. Chem.* **2000**, *65*, 4776–4778. (f) Pican, P.; Gaumont, A. C. *Chem. Commun.* **2005**, 2393–2395.
- (16) For Ni-catalyzed C–P bond formation processes, see: (a) Cai, D. W.; Payack, J. F.; Bender, D. R.; Hughes, D. L.; Verhoeven, T. R.; Reider, P. J. *J. Org. Chem.* **1994**, *59*, 7180–7181. (b) Clarke, M. L.; Orpen, A. G.; Pringle, P. G.; Turley, E. *Dalton Trans.* **2003**, 4393–4394.
- (17) For Cu-catalyzed C–P bond formation processes, see: (a) Ogawa, T.; Usuki, N.; Ono, N. *J. Chem. Soc., Perkin Trans. 1* **1998**, 2953–2958. (b) Gelman, D.; Jiang, L.; Buchwald, S. L. *Org. Lett.* **2003**, *5*, 2315–2318. (c) Van Allen, D.; Venkataraman, D. *J. Org. Chem.* **2003**, *68*, 4590–4593. (d) Tani, K.; Behenna, D. C.; McFadden, R. M.; Stoltz, B. M. *Org. Lett.* **2007**, *9*, 2529–2531. (e) Krout, M. R.; Mohr, J. T.; Stoltz, B. M. *Org. Synth.* **2009**, *86*, 181–193.
- (18) For the first example of microwave-assisted C–P coupling, see: (a) Stadler, A.; Kappe, C. O. *Org. Lett.* **2002**, *4*, 3541–3543. For a recent example, see: (b) Damian, K.; Clarke, M. L.; Copley, C. J. *Appl. Organomet. Chem.* **2009**, *23*, 272–276.

- (19) Initial reaction conditions were based on this microwave-assisted Suzuki–Miyaura coupling: Wawrzyniak, P.; Heinicke, J. *Tetrahedron Lett.* **2006**, *47*, 8921–8924.
- (20) Complete conversion of starting material was essential for purification, since the R_f values were almost identical.
- (21) Busacca, C. A.; Lorenz, J. C.; Grinberg, N.; Haddad, N.; Hrapchak, M.; Latli, B.; Lee, H.; Sabila, P.; Saha, A.; Sarvestani, M.; Shen, S.; Varsolona, R.; Wei, X.; Senanayake, C. H. *Org. Lett.* **2005**, *7*, 4277–4280.
- (22) Casey, C. P.; Paulsen, E. L.; Beuttenmueller, E. W.; Proft, B. R.; Matter, B. A.; Powell, D. J. *Am. Chem. Soc.* **1999**, *121*, 63–70.
- (23) (a) Orpen, A. G.; Brammer, L.; Allen, F. H.; Kennard, O.; Watson, D. G.; Taylor, R. *J. Chem. Soc., Dalton Trans.* **1989**, S1–S83. (b) Bringmann, G.; Wuzik, A.; Stowasser, R.; Rummey, C.; Gobel, L.; Stalke, D.; Pfeiffer, M.; Schenk, W. A. *Organometallics* **1999**, *18*, 5017–5021. (c) Geldbach, T. J.; Pregosin, P. S.; Albinati, A. *Organometallics* **2003**, *22*, 1443–1451. (d) Hermatschweller, R.; Pregosin, P. S.; Albinati, A.; Rizzato, S. *Inorg. Chim. Acta* **2003**, *354*, 90–93. (e) Geldbach, T. J.; Breher, F.; Gramlich, V.; Kumar, P. G. A.; Pregosin, P. S. *Inorg. Chem.* **2004**, *43*, 1920–1928. (f) Takemoto, S.; Oshio, S.; Shiromoto, T.; Matsuzaka, H. *Organometallics* **2005**, *24*, 801–804. (g) Takemoto, S.; Ogura, S.; Kamikawa, K.; Matsuzaka, H. *Inorg. Chim. Acta* **2006**, *359*, 912–916. (h) Shibasaki, T.; Komine, N.; Hirano, M.; Komiya, S. *J. Organomet. Chem.* **2007**, *692*, 2385–2394.
- (24) Muetterties, E. L.; Bleeke, J. R.; Wucherer, E. J.; Albright, T. A. *Chem. Rev.* **1982**, *82*, 499–525.
- (25) This pattern of ellipsoids appeared much less pronounced in the well-ordered structures of **13b** and **14b**.
- (26) For NMR data of 1,4-dibromonaphthalene in CDCl_3 , see: Cakmak, O.; Demirtas, I.; Balaydin, H. T. *Tetrahedron* **2002**, *58*, 5603–5609.
- (27) (a) Mann, B. E.; Taylor, B. F. In *13C NMR Data for Organometallic Compounds*; Academic Press: London, 1981. (b) Wheeler, D. E.; Hill, S. T.; Carey, J. M. *Inorg. Chim. Acta* **1996**, *249*, 157–161.
- (28) Vitorge, B.; Bieri, S.; Humam, M.; Christen, P.; Hostettmann, K.; Munoz, O.; Loss, S.; Jeannerat, D. *Chem. Commun.* **2009**, 950–952.
- (29) Kalinowski, H.-O.; Berger, S.; Braun, S. In *13C-NMR-Spektroskopie*; Georg Thieme Verlag: Stuttgart, Germany, 1984.
- (30) Müller, T. E.; Green, J. C.; Mingos, D. M. P.; Mcpartlin, C. M.; Whittingham, C.; Williams, D. J.; Woodroffe, T. M. *J. Organomet. Chem.* **1998**, *551*, 313–330.
- (31) The ^{13}C NMR spectrum of iron complex **8b** was misinterpreted in ref 4b. Spectral data of **8b** in C_6D_6 are therefore reported in the Experimental Section and in Table S3 (Supporting Information).
- (32) Tolman, C. A. *Chem. Rev.* **1977**, *77*, 313–348.
- (33) For an application to NHCs, see: Nolan, S. P.; Dorta, R.; Stevens, E. D.; Scott, N. M.; Costabile, C.; Cavallo, L.; Hoff, C. D. *J. Am. Chem. Soc.* **2005**, *127*, 2485–2495.
- (34) The σ -donor ability and the π -acceptor strength are the two main components of the net donating ability of phosphines.
- (35) For reviews, see: (a) Dias, P. B.; Depiedade, M. E. M.; Simoes, J. A. M. *Coord. Chem. Rev.* **1994**, *135*, 737–807. (b) Kühl, O. *Coord. Chem. Rev.* **2005**, *249*, 693–704. (c) Fey, N.; Orpen, A. G.; Harvey, J. N. *Coord. Chem. Rev.* **2009**, *253*, 704–722. (d) Glorius, F.; Dröge, T. *Angew. Chem., Int. Ed.* **2010**, *49*, 6940–6952.
- (36) For scales based on various metal carbonyl complexes and their calibration with respect to TEP, see ref 35b.
- (37) Selected theoretical studies: (a) Gusev, D. G. *Organometallics* **2009**, *28*, 6458–6461. (b) Gusev, D. G. *Organometallics* **2009**, *28*, 763–770.
- (38) Tolman, C. A. *J. Am. Chem. Soc.* **1970**, *92*, 2953–2955.
- (39) Gassman, P. G.; Mickelson, J. W.; Sowa, J. R. *J. Am. Chem. Soc.* **1992**, *114*, 6942–6944.
- (40) For criticisms of Tolman's assumption, see: (a) Bartik, T.; Himmler, T.; Schulte, H. G.; Seevogel, K. *J. Organomet. Chem.* **1984**, *272*, 29–41. (b) Reference 35c.
- (41) Perrin, D. D.; Armarego, W. L. F. *Purifications of Laboratory Chemicals*; Pergamon Press: Oxford, U.K., 1988.
- (42) Ukai, T.; Kawazura, H.; Ishii, Y.; Bonnet, J. J.; Ibers, J. A. *J. Organomet. Chem.* **1974**, *65*, 253–266.
- (43) Puddephatt, R. J.; Brandys, M. C.; Jennings, M. C. *J. Chem. Soc., Dalton Trans.* **2000**, 4601–4606.
- (44) (a) Hays, H. R. *J. Org. Chem.* **1968**, *33*, 3690–3694. (b) Busacca, C. A.; Lorenz, J. C.; Grinberg, N.; Haddad, N.; Hrapchak, M.; Latli, B.; Lee, H.; Sabila, P.; Saha, A.; Sarvestani, M.; Shen, S.; Varsolona, R.; Wei, X. D.; Senanayake, C. H. *Org. Lett.* **2005**, *7*, 4277–4280. (c) Casey, C. P.; Paulsen, E. L.; Beuttenmueller, E. W.; Proft, B. R.; Petrovich, L. M.; Matter, B. A.; Powell, D. R. *J. Am. Chem. Soc.* **1997**, *119*, 11817–11825.
- (45) Altomare, A.; Cascarano, G.; Giacovazzo, C.; Guagliardi, A.; Burla, M. C.; Polidori, G.; Camalli, M. *J. Appl. Crystallogr.* **1994**, *27*, 435.
- (46) Altomare, A.; Burla, M. C.; Camalli, M.; Cascarano, G. L.; Giacovazzo, C.; Guagliardi, A.; Moliterni, A. G. G.; Polidori, G.; Spagna, R. *J. Appl. Crystallogr.* **1999**, *32*, 115–119.
- (47) Palatinus, L.; Chapuis, G. *J. Appl. Crystallogr.* **2007**, 786–790.
- (48) Betteridge, P. W.; Carruthers, J. R.; Cooper, R. I.; Prout, K.; Watkin, D. J. *J. Appl. Crystallogr.* **2003**, *36*, 1487.
- (49) *XTAL3.2 Reference Manual*; Hall, S. R., Flack, H. D., Stewart, J. M., Eds.; Universities of Western Australia, Geneva, and Maryland, 1992.
- (50) *cis*-bis(μ -chloro)bis[1-((1*S*)-1-(dimethylamino)ethyl)naphthalen-2-yl]dipalladium(II) was prepared according to a literature procedure: (a) Allen, D. G.; McLaughlin, G. M.; Robertson, G. B.; Steffen, W. L.; Salem, G.; Wild, S. B. *Inorg. Chem.* **1982**, *21*, 1007–1014. (b) Hockless, D. C. R.; Gugger, P. A.; Leung, P. H.; Mayadunne, R. C.; Pabel, M.; Wild, S. B. *Tetrahedron* **1997**, *53*, 4083–4094.
- (51) In some cases, the reaction mixture turned rapidly black after the completed consumption of $\text{Ni}(\text{cod})_2$ (as indicated by the color change; precipitation of $\text{Ni}(0)$). This color change had no influence on the IR spectra.
- (52) Inverse reaction order led to significant formation of $\text{Ni}(\text{CO})_2(\text{Ph}_3\text{P})_2$.